Supporting Information

Reductive Hydroformylation of Methyl 10-Undecenoate Catalyzed by a Rhodium/Trialkylamine Combination Associated with Silica: A New Step Towards a Simple, Robust and Recyclable Catalytic System

Abdelhadi Zouhair,[a,b] Michel Ferreira,[b] Hervé Bricout,[b] Nicolas Kania,[b] Bastien Léger,[b] Jérémy Ternel,[b] Anne Ponchel,[b] Mohammed Lahcini,[a,c] Sébastien Tilloy[b] and Eric Monflier[b]

a. IMED-Lab, Faculty of Sciences and Techniques, Cadi Ayyad University (UCA), Avenue Abdelkrim Elkhattabi, B.P 549, 40000 Marrakech, Morocco

b. Univ. Artois, CNRS, Centrale Lille, Univ. Lille, UMR 8181, Unité de Catalyse et Chimie du Solide (UCCS), rue Jean Souvraz, SP 18, 62300 Lens, France

c. College of Chemical Sciences and Engineering (CCSE), Chemical & Biochemical Sciences, Green Process Engineering (CBS), Mohammed VI Polytechnic University (UM6P), Lot 660 Hay Moulay Rachid, Ben Guerir, Morocco

Table of contents

I. Experimental results S1

1. Influence of amine structure on catalytic performance and rhodium concentration in solution S1
2. Photographs of silica materials after reaction with and without amine addition S2
3. Recycling experiments without amine addition S3
4. Recycling experiments with TEA addition S4
   a. Conversions and selectivities obtained over 6 h S4
   b. Conversions and selectivities obtained over 24 h S5
   c. Evolution of Rh content present in the reactor and $TOF_{alcohols}$ over runs and cumulative time S6
5. Hydrated silica S7
6. Thermally treated silica S8
7. Influence of rhodium and amine concentration S9
8. Influence of solvent S10
9. Comparison with literature-reported catalytic systems S11
10. Reductive hydroformylation of methyl 10-undecenoate under neat conditions S13
11. SEM and EDX experiments S14
    a. Silica material after the first run (Rh_1) S15
    b. Silica material after 10 recycling cycles (Rh_10) S16
12. TEM and HAADF-STEM analysis S20
13. HAADF-STEM analysis of the thermally treated catalytic material (Rh_TT) S25
14. XPS analysis of silica material after the first run (Rh_1) S26
15. Evaluation of Rh content in liquid phase S27
    a. Under various conditions S27
    b. At different reaction times S28
16. Sheldon's hot filtration test S29
17. Recycling experiments with TEA addition over 6 h S31
18. Kinetic follow-up of UM reductive hydroformylation in the presence of silica support S33
19. Supplementary Experiences S34
    a. Influence of silica particle size on the HHM reaction and Rh distribution S34
    b. Influence of silica loading S36

c. Influence of the organic phase volume S38
II. Experimental and analytical procedures S39
1. General information S39
2. Synthesis and characterization of potassium *N,N*-dimethyltaurinate (K-DMT) and PEMIM-PF_6 ..... S39
3. Physical-chemical characterization S40
4. Preparation of thermal treatment of silica S41
5. Preparation of various hydrated silica S42
6. Catalytic tests in batch process S42
7. Recycling experiments without amine addition S43
8. Recycling experiments with amine addition S43
9. Determination of conversion, yields, and l/b ratios for the catalytic experiments S43
III. References S44

I. Experimental results

1. Influence of amine structure on catalytic performance and rhodium concentration in solution

Table S1. Rhodium catalyzed reductive hydroformylation of MU in the presence of silica and various trialkylamines[a]

Entry	Ligand	Conv.[b] (%)	$Y_{(Ald)}$[c] (%) [*l*/*b*][d]	$Y_{(Alc)}$[c] (%) [*l*/*b*][e]	Global [*l*/*b*][f]	$Y_{(Iso)}$[c] (%)	$Y_{(Sat)}$[c] (%)	Rh content[g] (%)
1	No amine	100	94 [1.0]	0	[1.0]	0	6	53.3
2	TOA	100	86 [1.6]	0	[1.6]	9	5	8.9
3	TBA	98	73 [1.8]	0	[1.8]	20	5	7.8
4	TIBA	100	91 [1.0]	0	[1.0]	0	9	14.0
5	DIPEA	62	41 [1.7]	6 [1.7]	[1.7]	11	4	3.4
6	DMOA	99	61 [1.5]	16 [3.0]	[1.8]	18	4	6.3
7	TEA	68	22 [1.0]	27 [2.5]	[1.7]	17	2	3.2
8	TEOA	81	40 [1.4]	22 [3.2]	[1.8]	17	2	3.3
9	DMEA	81	22 [1.0]	37 [2.6]	[1.8]	20	2	3.4
10	DMEOA	98	5 [0.7]	74 [2.0]	[1.9]	15	4	3.6
11	K-DMT	99	13 [0.4]	68 [2.4]	[1.8]	14	4	5.1
12	PEMIM-PF_6	100	25 [0.3]	69 [2.0]	[1.2]	5	1	4.2

[a]Reaction conditions: $Rh(acac)(CO)_2$: 0.023 mmol (6 mg); Amine: 2.3 mmol (100 eq.); MU: 5.75 mmol (250 eq.); SiO_2(2 wt% water): 1.2 g; heptane: 10.32-x mL where x is the added volume of amine; 80 °C; 80 bar CO/H_2 (1:1); 6 h. [b]Methyl 10-undecenoate conversion. [c]Y(X) = yield in (X); (Ald) = aldehydes; (Alc) = alcohols; (Iso) = methyl 10-undecenoate isomers; and (Sat) = saturated compound = methyl undecanoate. [d]Linear to branched ratio for aldehydes. [e]Linear to branched ratio for alcohols. [f]Global linear to branched ratio. [g]Rh content detected in the liquid phase after reaction.

2. Photographs of silica materials after reaction with and without amine addition

Entry	Liquid phase	Solid phase
Without amine		
With triethylamine (TEA)		

Fig. S1. Photographs of liquid phases and silica materials after reaction with and without TEA addition.

3. Recycling experiments without amine addition

Table S2. Recycling experiment with various trialkylamines and without addition of amines between runs[a]

Ligand	Recycling run	Conv.[b] (%)	$Y_{(Ald)}$[c] (%) [*l/b*][d]	$Y_{(Alc)}$[c] (%) [*l/b*][e]	Global [*l/b*][f]	$Y_{(Iso)}$[c] (%)	$Y_{(Sat)}$[c] (%)	Rh content[g] (%)
TEA	Run 1	68	22 [1.0]	27 [2.5]	[1.7]	17	2	3.2
	Run 2	100	69 [1.9]	10 [4.0]	[2.0]	16	5	4.1
	Run 3	100	77 [1.7]	7 [6.0]	[1.8]	12	4	4.5
DMEA	Run 1	81	22 [1.0]	37 [2.6]	[1.8]	20	2	3.4
	Run 2	100	67 [1.4]	17 [4.0]	[1.6]	15	1	3.6
	Run 3	100	82 [1.2]	11 [4.0]	[1.4]	5	2	3.7
DMEOA	Run 1	98	5 [0.7]	74 [2.0]	[1.9]	15	4	3.6
	Run 2	96	34 [1.3]	37 [3.1]	[2.0]	18	7	5.4
	Run 3	98	59 [1.5]	19 [5.3]	[2.0]	18	2	4.8
K-DMT	Run 1	99	13 [0.4]	68 [2.4]	[1.8]	14	4	5.1
	Run 2	100	13 [0.3]	75 [2.6]	[1.8]	9	3	4.0
	Run 3	99	21 [0.5]	66 [3.1]	[1.9]	10	2	4.5
	Run 4	99	31 [0.9]	49 [3.5]	[2.0]	15	4	4.8
	Run 5	99	38 [1.2]	38 [3.8]	[2.0]	18	5	4.5
PEMIM-PF_6	Run 1	100	25 [0.3]	69 [1.8]	[1.3]	5	1	4.2
	Run 2	99	36 [0.6]	57 [2.0]	[1.2]	5	1	4.4
	Run 3	99	53 [0.9]	37 [2.5]	[1.3]	8	1	4.6

[a]Reaction conditions for the first run: $Rh(acac)(CO)_2$: 0.023 mmol (6 mg); Amine: 2.3 mmol (100 eq.); MU: 5.75 mmol (250 eq.); SiO_2 (2 wt% water): 1.2 g; heptane: 10.32-x mL where x is the added volume of amine; 80 °C; 80 bar CO/H_2 (1:1); 6 h. Run N was conducted with the solid phase of run number N-1, after washing with 3×7 mL of heptane and addition of a fresh mixture of MU (5.75 mmol)/heptane (10 mL). [b]Methyl 10-undecenoate conversion. [c]Y(X) = yield in (X); (Ald) = aldehydes; (Alc) = alcohols; (Iso) = methyl 10-undecenoate isomers; and (Sat) = saturated compound = methyl undecanoate. [d]Linear to branched ratio for aldehydes. [e]Linear to branched ratio for alcohols. [f]Global linear to branched ratio. [g]Rh content detected in the liquid phase after reaction.

4. Recycling experiments with TEA addition

a. Conversions and selectivities obtained over 6 h ($Rh(acac)(CO)_2$: 0.023 mmol (6 mg) and TEA: 2.3 mmol (100 eq.))

Table S3. Recycling experiment with addition of TEA between each run over 6 h[a]

Run	Conv.[b] (%)	$Y_{(Ald)}$[c] (%) [*l/b*][d]	$Y_{(Alc)}$[c] (%) [*l/b*][e]	Global [*l/b*][f]	$Y_{(Iso)}$[c] (%)	$Y_{(Sat)}$[c] (%)	Rh content[g] (%)
1	68	22 [1.0]	27 [2.5]	[1.7]	17	2	3.2
2	77	22 [1.0]	37 [3.0]	[2.0]	16	2	3.6
3	77	21 [1.0]	37 [4.0]	[2.0]	16	3	3.5
4	75	21 [1.2]	35 [3.7]	[2.3]	16	3	3.6
5	76	23 [1.2]	34 [3.6]	[2.2]	17	2	3.9
6	74	23 [1.2]	32 [3.4]	[2.1]	16	3	3.4
7	75	26 [1.3]	29 [3.7]	[2.1]	16	4	3.4
8	75	28 [1.5]	29 [3.7]	[2.2]	15	3	3.8
9	73	27 [1.4]	28 [3.7]	[2.1]	15	3	3.8
10	69	28 [1.5]	26 [4.0]	[2.3]	13	2	3.1
11	69	29 [1.6]	26 [4.0]	[1.7]	12	2	3.5

[a]Reaction conditions for the first run: $Rh(acac)(CO)_2$: 0.023 mmol (6 mg); TEA: 2.3 mmol (100 eq.); MU: 5.75 mmol (250 eq.); SiO_2 (2 wt% water): 1.2 g; heptane: 10 mL; 80 °C; 80 bar CO/H_2 (1:1); 6 h. Run N was conducted with the solid phase of run number N-1, after washing with 3×7 mL of heptane and addition of a fresh mixture of MU (5.75 mmol)/heptane (10 mL)/TEA (2.3 mmol). [b]Methyl 10-undecenoate conversion. [c]Y(X) = yield in (X); (Ald) = aldehydes; (Alc) = alcohols; (Iso) = methyl 10-undecenoate isomers; and (Sat) = saturated compound = methyl undecanoate. [d]Linear to branched ratio for aldehydes. [e]Linear to branched ratio for alcohols. [f]Global linear to branched ratio. [g]Rh content detected in the liquid phase after reaction.

b. Conversions and selectivities obtained over 24 h ($Rh(acac)(CO)_2$: 0.023 mmol (6 mg) and TEA: 2.3 mmol (100 eq.))

Table S4. Recycling experiment with addition of TEA between each run[a]

Run	Conv.[b] (%)	$Y_{(Ald)}$[c] (%) [*l/b*][d]	$Y_{(Alc)}$[c] (%) [*l/b*][e]	Global [*l/b*][f]	$Y_{(Iso)}$[c] (%)	$Y_{(Sat)}$[c] (%)	Rh content[g] (%)
1	100	3 [0]	94 [1.1]	[1.0]	0	3	3.3
2	100	4 [0]	94 [1.4]	[1.1]	0	2	3.4
3	100	3 [0]	95 [1.3]	[1.1]	0	2	3.6
4	100	2 [0]	97 [1.5]	[1.2]	0	1	3.7
5	100	4 [0]	94 [1.3]	[1.1]	0	2	3.8
6	100	5 [0]	94 [1.4]	[1.2]	0	1	3.3
7	100	7 [0]	92 [1.4]	[1.2]	0	1	3.5
8	100	9 [0.1]	89 [1.4]	[1.2]	1	1	3.7
9	100	13 [0.1]	86 [1.7]	[1.3]	0	1	3.9
10	100	16 [0.1]	81 [1.8]	[1.2]	2	1	4.4
11	100	15 [0.1]	82 [1.8]	[1.3]	2	1	4.1

[a]Reaction conditions for the first run: $Rh(acac)(CO)_2$: 0.023 mmol (6 mg); TEA: 2.3 mmol (100 eq.); MU: 5.75 mmol (250 eq.); SiO_2 (2 wt% water): 1.2 g; heptane: 10 mL; 80 °C; 80 bar CO/H_2 (1:1); 24 h. Run N was conducted with the solid phase of run number N-1, after washing with 3×7 mL of heptane and addition of a fresh mixture of MU (5.75 mmol)/heptane (10 mL)/TEA(2.3 mmol). [b]Methyl 10-undecenoate conversion. [c]Y(X) = yield in (X); (Ald) = aldehydes; (Alc) = alcohols; (Iso) = methyl 10-undecenoate isomers; and (Sat) = saturated compound = methyl undecanoate. [d]Linear to branched ratio for aldehydes. [e]Linear to branched ratio for alcohols. [f]Global linear to branched ratio. [g]Rh content detected in the liquid phase after reaction.

c. Evolution of Rh content present in the reactor and $TOF_{alcohols}$ over runs and cumulative time

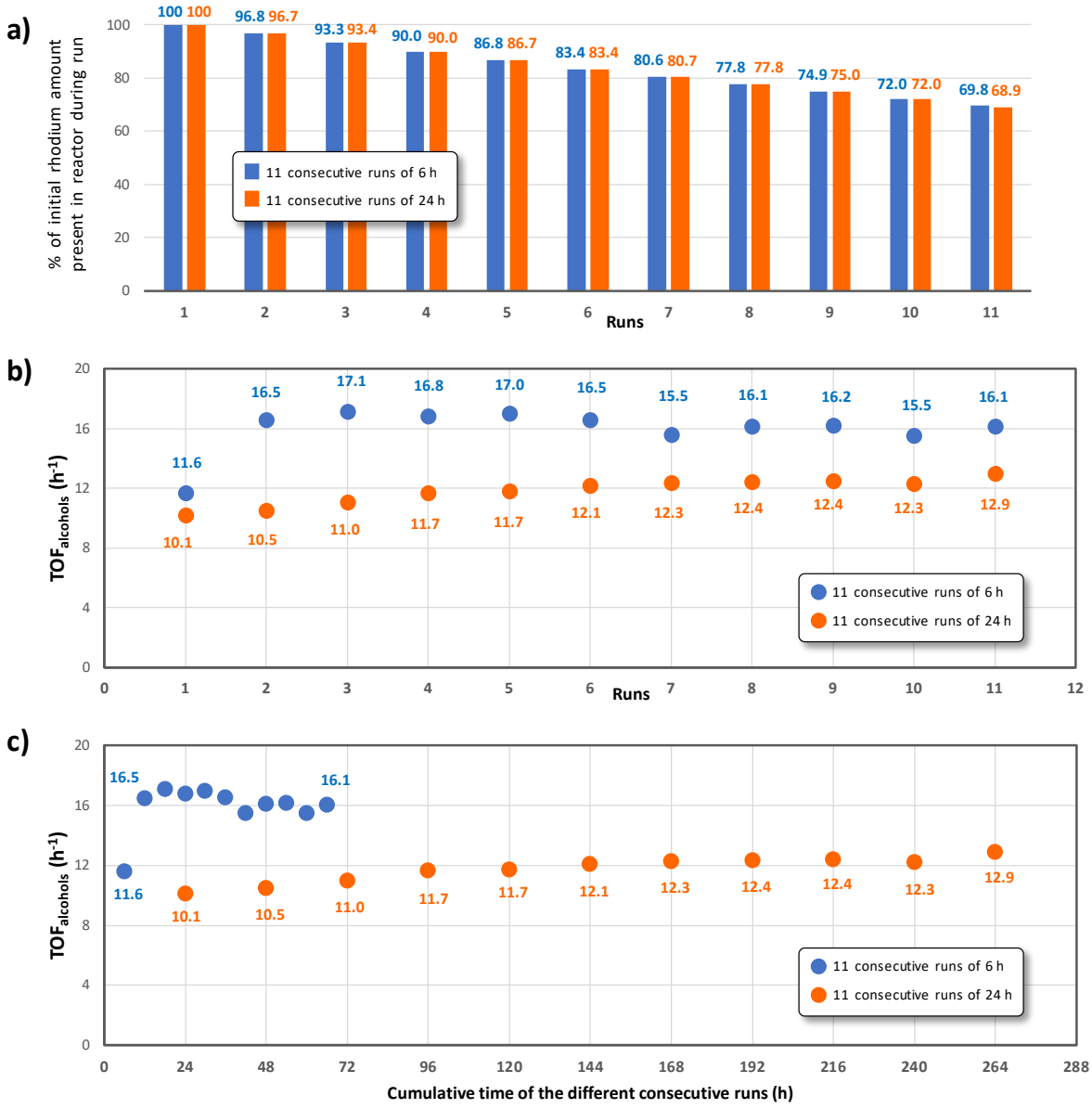

Fig. S2. Rh content present in the reactor for each run over 6 or 24 hours (a), and $TOF_{alcohols}$ evolution over (b) different recycling runs and (c) cumulative reaction time.

5. Hydrated silica

Table S5. Rhodium-catalyzed reductive hydroformylation of MU in the presence of silica with different hydration degrees[a]

Entry	Silica (wt% H_2O)	Conv.[b] (%)	$Y_{(Ald)}$[c] (%) [*l/b*][d]	$Y_{(Alc)}$[c] (%) [*l/b*][e]	Global [*l/b*][f]	$Y_{(Iso)}$[c] (%)	$Y_{(Sat)}$[c] (%)	Rh content[g] (%)
1	0.6	63	20 [1.0]	20 [1.3]	[1.1]	22	1	2.3
2	2.0	68	22 [1.0]	27 [2.5]	[1.7]	17	2	3.2
3	7.4	69	16 [1.1]	37 [3.1]	[1.9]	14	2	3.4
4	44	96	36 [0.8]	39 [3.3]	[1.5]	20	1	5.2
5	54	100	61 [0.8]	36 [2.0]	[1.1]	0	3	76.5
6[h]	-	100	49 [0.7]	46 [1.9]	[1.1]	0	5	-

[a]Reaction conditions: $Rh(acac)(CO)_2$: 0.023 mmol (6 mg); TEA: 2.3 mmol (100 eq.); MU: 5.75 mmol (250 eq.); SiO_2 (X wt% H_2O): Dry SiO_2 (1.18 g) + water (1.18 X/(100-X) g); heptane: 10 mL; 80 °C; 80 bar CO/H_2 (1:1); 6 h. [b]Methyl 10-undecenoate conversion. [c]Y(X) = yield in (X); (Ald) = aldehydes; (Alc) = alcohols; (Iso) = methyl 10-undecenoate isomers; and (Sat) = saturated compound = methyl undecanoate. [d]Linear to branched ratio for aldehydes. [e]Linear to branched ratio for alcohols. [f]Global linear to branched ratio. [g]Rh content detected in the liquid phase after reaction. [h]Reaction conducted without silica.

6. Thermally treated silica

Table S6. Textural characteristics of thermally treated silica

Silica@Treatment temperature	S_{BET} ($m^2.g^{-1}$)	Average pore size (nm)	Total pore volume ($cm^3.g^{-1}$)
Silica (0.6 wt% H_2O)	430	5.35	0.73
Silica@500 °C	450	5.45	0.75
Silica@600 °C	455	5.38	0.74
Silica@700 °C	451	5.32	0.73
Silica@1000 °C	≈ 0.5	-	-

Table S7. Rhodium-catalyzed reductive hydroformylation of MU in the presence of thermally treated silica[a]

Entry	Silica@Treatment temperature	Conv.[b] (%)	$Y_{(Ald)}$[c] (%) [*l/b*][d]	$Y_{(Alc)}$[c] (%) [*l/b*][e]	Global [*l/b*][f]	$Y_{(Iso)}$[c] (%)	$Y_{(Sat)}$[c] (%)	Rh content[g] (%)
1	Silica (0.6 wt% H_2O)	63	20 [1.0]	20 [1.3]	[1.1]	22	1	2.3
2	Silica@500 °C	78	20 [1.3]	38 [2.9]	[2.1]	17	3	3.7
3	Silica@600 °C	83	32 [1.4]	28 [3.3]	[2.0]	21	2	4.7
4	Silica@700 °C	85	31 [1.3]	31 [3.7]	[2.1]	21	2	5.9
5	Silica@1000 °C	100	47 [0.7]	49 [1.9]	[1.1]	0	4	90

[a]Reaction conditions: $Rh(acac)(CO)_2$: 0.023 mmol (6 mg); TEA: 2.3 mmol (100 eq.); MU: 5.75 mmol (250 eq.); SiO_2@T °C: 1.2 g; heptane: 10 mL; 80 °C; 80 bar CO/H_2 (1:1); 6 h. [b]Methyl 10-undecenoate conversion. [c]Y(X) = yield in (X); (Ald) = aldehydes; (Alc) = alcohols; (Iso) = methyl 10-undecenoate isomers; and (Sat) = saturated compound = methyl undecanoate. [d]Linear to branched ratio for aldehydes. [e]Linear to branched ratio for alcohols. [f]Global linear to branched ratio. [g]Rh content detected in the liquid phase after reaction.

7. Influence of rhodium and amine concentration

Table S8. Influence of rhodium and amine concentrations on reductive hydroformylation of MU in the presence of silica[a]

Entry	n_{Rh} (µmol)	n_{TEA} (mmol)	TEA/Rh	Conv.[b] (%)	$Y_{(Ald)}$[c] (%) [*l*/*b*][d]	$Y_{(Alc)}$[c] (%) [*l*/*b*][e]	Global [*l*/*b*][f]	$Y_{(Iso)}$[c] (%)	$Y_{(Sat)}$[c] (%)	Rh content[g] (%)
1	1.15	0.11	100	100	93 [1.2]	0 [-]	[1.2]	7	0	52.0
2	1.15	2.3	2000	25	21 [1.8]	1 [-]	[1.8]	3	0	18.0
3	1.15	4.6	4000	27	15 [2.0]	3 [4.0]	[2.4]	8	1	11.0
4	1.15	9.2	8000	26	15 [2.0]	5 [6.0]	[3.0]	5	1	12.0
5	3.83	2.3	600	46	29 [1.9]	9 [6.0]	[2.3]	7	1	7.5
6	3.83	4.6	1200	46	24 [1.5]	12 [4.0]	[2.0]	9	1	8.0
7	3.83	9.2	2400	49	19 [1.4]	18 [3.0]	[2.0]	11	1	8.0
8	11.5	1.15	100	59	41 [2.0]	7 [3.0]	[2.1]	10	1	2.9
9	11.5	2.3	200	56	26 [1.4]	15 [3.3]	[1.9]	14	1	5.0
10	11.5	4.6	400	73	17 [1.0]	38 [2.9]	[2.0]	17	1	3.6
11	11.5	9.2	800	86	12 [0.8]	58 [2.5]	[2.0]	14	2	5.0
12	23	2.3	100	68	22 [1.0]	27 [2.5]	[1.7]	17	2	3.2
13	23	4.6	200	80	14 [1.0]	47 [2.5]	[2.0]	18	1	4.4
14	23	9.2	400	89	6 [1.0]	63 [2.2]	[2.0]	19	1	5.3
15	23	13.8	600	92	4 [1.0]	70 [2.2]	[2.0]	17	1	3.8
16	46	2.3	50	94	13 [0.9]	56 [2.7]	[2.0]	24	1	3.1
17	46	4.6	100	98	4 [0.5]	72 [2.0]	[1.9]	21	1	3.2
18	46	9.2	200	100	1 [1.0]	88 [1.7]	[1.7]	10	1	2.4

[a]Reaction conditions: $Rh(acac)(CO)_2$: x µmol; TEA: y mmol; MU: 5.75 mmol; SiO_2(2 wt% water): 1.2 g; heptane: 10.32-x mL where x is the added volume of TEA; 80°C; 80 bar CO/H_2 (1:1); 6 h. [b]Methyl 10-undecenoate conversion. [c]Y(X) = yield in (X); (Ald) = aldehydes; (Alc) = alcohols; (Iso) = methyl 10-undecenoate isomers; and (Sat) = saturated compound = methyl undecanoate. [d]Linear to branched ratio for aldehydes. [e]Linear to branched ratio for alcohols. [f]Global linear to branched ratio. [g]Rh content detected in the liquid phase after reaction.

8. Influence of solvent

Table S9. Influence of solvent nature on reductive hydroformylation of MU in the presence of silica[a]

Entry	Solvent	Conv.[b] (%)	$Y_{(Ald)}$[c] (%) [*l*/*b*][d]	$Y_{(Alc)}$[c] (%) [*l*/*b*][e]	Global [*l*/*b*][f]	$Y_{(Iso)}$[c] (%)	$Y_{(Sat)}$[c] (%)	Rh content[g] (%)
1	Dodecane	65	15 [0.9]	30 [2.1]	[1.6]	20	0	1.9
2	Heptane	68	22 [1.0]	27 [2.5]	[1.7]	17	2	3.2
3	Pinane	80	23 [1.3]	33 [2.6]	[1.9]	24	0	2.8
4	*p*-Cymene	97	24 [0.9]	46 [2.7]	[1.8]	27	0	3.7
5	DMC	100	9 [0.1]	79 [2.0]	[1.6]	12	0	3.8
6	Anisole	100	7 [0.1]	86 [1.8]	[1.5]	7	0	4.5
7	2-MeTHF	100	50 [1.4]	27 [3.3]	[1.8]	22	1	9.7
8	MIBK	95	54 [1.8]	28 [3.6]	[2.2]	12	1	54.0
9	Cyrene	72	62 [1.6]	4 [1.6]	[1.6]	5	1	44.0
10	GVL	14	8 [2.0]	0 [-]	[2.0]	6	0	95.0

[a]Reaction conditions: $Rh(acac)(CO)_2$: 0.023 mmol (6 mg); TEA: 2.3 mmol (100 eq.); MU: 5.75 mmol (250 eq.); SiO_2 (2 wt% water): 1.2 g; Solvent: 10 mL; 80 °C; 80 bar CO/H_2 (1:1); 6 h. [b]Methyl 10-undecenoate conversion. [c]Y(X) = yield in (X); (Ald) = aldehydes; (Alc) = alcohols; (Iso) = methyl 10-undecenoate isomers; and (Sat) = saturated compound = methyl undecanoate. [d]Linear to branched ratio for aldehydes. [e]Linear to branched ratio for alcohols. [f]Global linear to branched ratio. [g]Rh content detected in the liquid phase after reaction.

9. Comparison with literature-reported catalytic systems

Table S10. Comparison of various biphasic and heterogeneous catalysts

System type	Substrate	C=C/Rh[a]	Solvent	T (°C)	P (bar)	CO:H_2 ratio	t (h)	Y_{alc}[b] (%)	$TOF_{alcohols}$ (h^{-1})	Rh content[c] (%)	Ref.
Liquid-liquid biphasic system	1-Hexene	300	*n*-Dodecane	100	50	1:1	3	25	25	<10	[1]
								45[d]	45	ND[e]	
								50[d]	50		
								52[d]	52		
								64[d]	64		
								50[d]	50		
	1-Octene	840	*n*-Dodecane	100	60	1:1	5	50	82	ND[e]	[2]
		100	DMAE	80	90	1:2	1.5	64	43	ND[e]	[3]
	10-Methyl undecenoate	250	Heptane	80	80	1:1	24	70	7	4.1	[4]
		250		80	80	1:1	24	57	6	2.2	[5]
Solid-liquid system	1-Hexene	350	Toluene	100	50	1:1	4	7	6	ND[e]	[1]
								9[d]	8		
								4[d]	4		
								1[d]	1		
		640	Toluene + benzene	100	50	1:1	17	99	36	ND[e]	[6]
		300		100	50	1:1	17	97	17	ND[e]	[7]
		3200	Toluene	120	100	1:1	24	27	36	3.6	[8]
		492	Toluene	120	120	1:1	5	71	70	3	
								34[d]	34	2	
								100[d]	98	1	
		120	Toluene	120	120	1:1	5	100	24	4	
		214						48[d]	21	2	
		214						62[d]	27	2	
		273	Toluene	120	120	1:1	5	75	41	4	
								32[d]	18	2	
								33[d]	18	<0.1	
	1-Octene	600	Toluene	80	60	1:3	12	92	46	ND[e]	[9]

		1000	1-Octene	100	75	1:2	4	15	38	4	[10]
								18[d]	45	10	
								15[d]	38	4	
								13[d]	33	3.5	
								11[d]	28	2.8	
								10[d]	25	2	
								8[d]	20	2.5	
								8[d]	20	2	
								9[d]	23	2	
								8[d]	20	2	
								7[d]	18	2	
								7[d]	18	2	
								7[d]	18	2	
	10-Methyl Undecenoate	250	Anisole	80	80	1:1	6	86	36	4.5	**This work**
			DMC					79	33	3.8	
			p-Cymene					46	19	3.7	
			Pinane					33	14	2.8	
			Heptane					27	12	3.2	
	10-Methyl Undecenoate[f]	500	Heptane	80	80	1:1	6	58	49	5	

[a]Substrate/catalyst ratio. [b]Yield of alcohol. [c]Rh content detected in the organic phase. [d]Recycling runs. [e]Not determined. [f]Reaction described in Table S8 (entry 11), reaction conditions: $Rh(acac)(CO)_2$: 11.5 µmol (3.0 mg); TEA: 9.2 mmol (800 eq.); MU: 5.75 mmol (500 eq.); SiO_2 (2 wt% water): 1.2g; heptane: 9.03 mL; 80 °C; 80 bar CO/H_2 (1:1); 6 h.

10. Reductive hydroformylation of methyl 10-undecenoate under neat conditions

Table S11. Kinetic follow-up of the MU HHM catalyzed by the Rh/TEA/Silica under neat conditions[a]

Entry	Time (h)	Conv.[b] (%)	$Y_{(Ald)}$[c] (%) [*l/b*][d]	$Y_{(Alc)}$[c] (%) [*l/b*][e]	Global [*l/b*][f]	$Y_{(Iso)}$[c] (%)	$Y_{(Sat)}$[c] (%)	$TOF_{alcohols}$ (h^{-1})	Rh content[g] (%)
1	6	52	25 [1.9]	9 [2.0]	[1.9]	16	2	14	ND[h]
2	24	99	29 [1.0]	43 [2.1]	[1.6]	24	3	17	ND[h]
3	48	100	7 [0.1]	76 [1.6]	[1.4]	14	3	15	6.9

[a]Reaction conditions: $Rh(acac)(CO)_2$: 0.046 mmol (12 mg); TEA: 2.3 mmol (50 eq.); MU: 43.85 mmol (953 eq.); SiO_2 (2 wt% water): 1.2 g; 80 °C; 80 bar CO/H_2 (1:1). [b]Methyl 10-undecenoate conversion. [c]Y(X) = yield in (X); (Ald) = aldehydes; (Alc) = alcohols; (Iso) = methyl 10-undecenoate isomers; and (Sat) = saturated compound = methyl undecanoate. [d]Linear to branched ratio for aldehydes. [e]Linear to branched ratio for alcohols. [f]Global linear to branched ratio. [g]Rh content detected in the liquid phase after reaction. [h]Not determined.

11. SEM and EDX experiments

- **Samples designation**

The sample abbreviations are defined as follows:

The silica recovered after the first reaction cycle (Run 1) at 6 hours, as reported in **table S3**, was divided into two portions:

i) The first portion was analyzed as received and is designated **Rh_1**.

ii) The second portion was subjected to a thermal treatment at 600 °C for 2 hours under a nitrogen atmosphere and is designated **Rh_TT**.

The third sample, **Rh_10**, was obtained by recovering the silica after ten consecutive recycling cycles corresponding to the same series as Rh_1 (Run 11, **Table S3**).

This designation was applied consistently across all characterization techniques, including SEM, TEM, HAADF-STEM, and XPS.

a. Silica material after the first run (Rh_1)

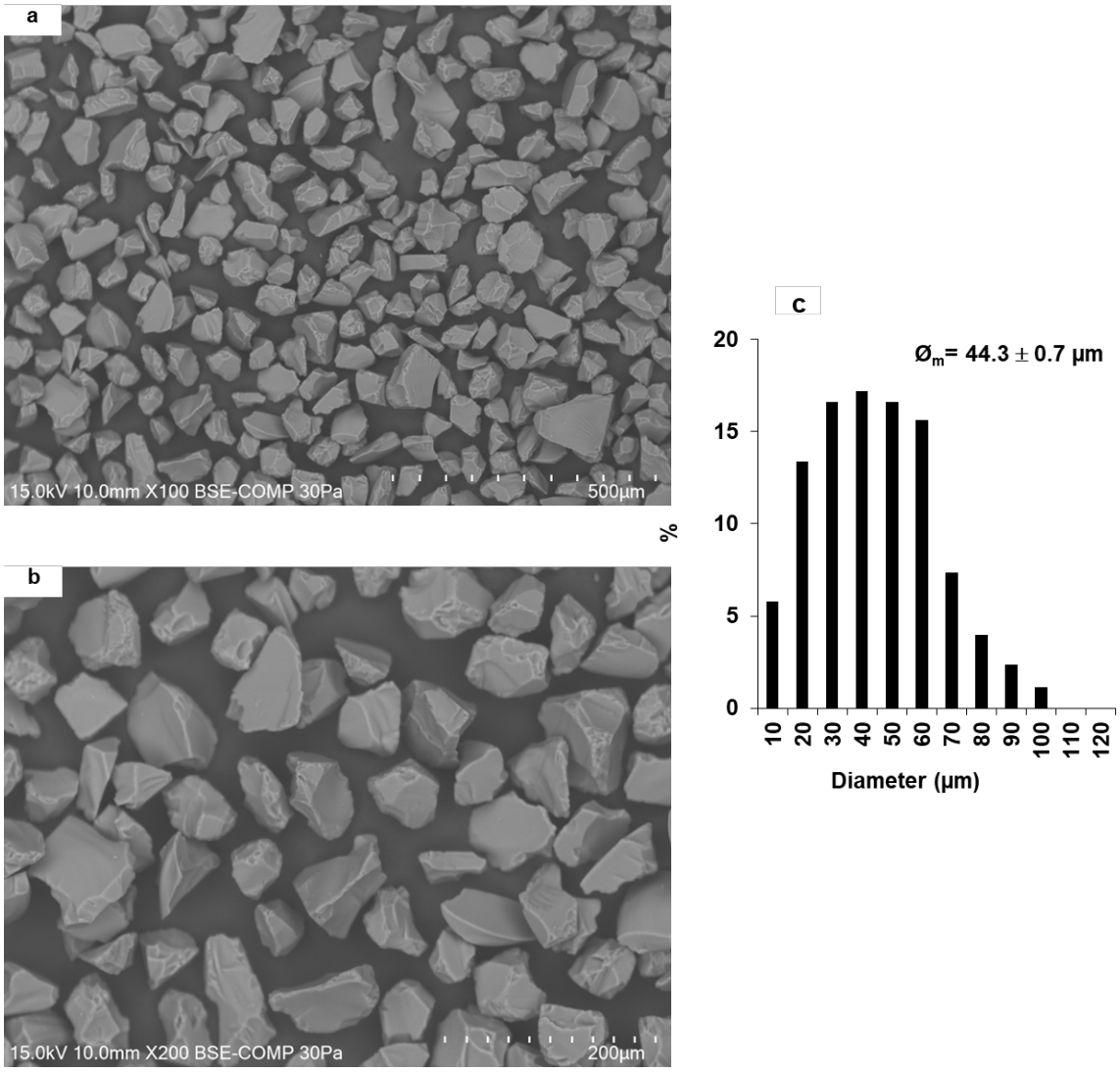

Fig. S3. SEM images of **Rh_1 sample** at a magnification of × 100 (**a**), × 200 (**b**), and their particle size distribution (c) determined using Fiji/ImageJ

b. Silica material after 10 recycling cycles (Rh_10)

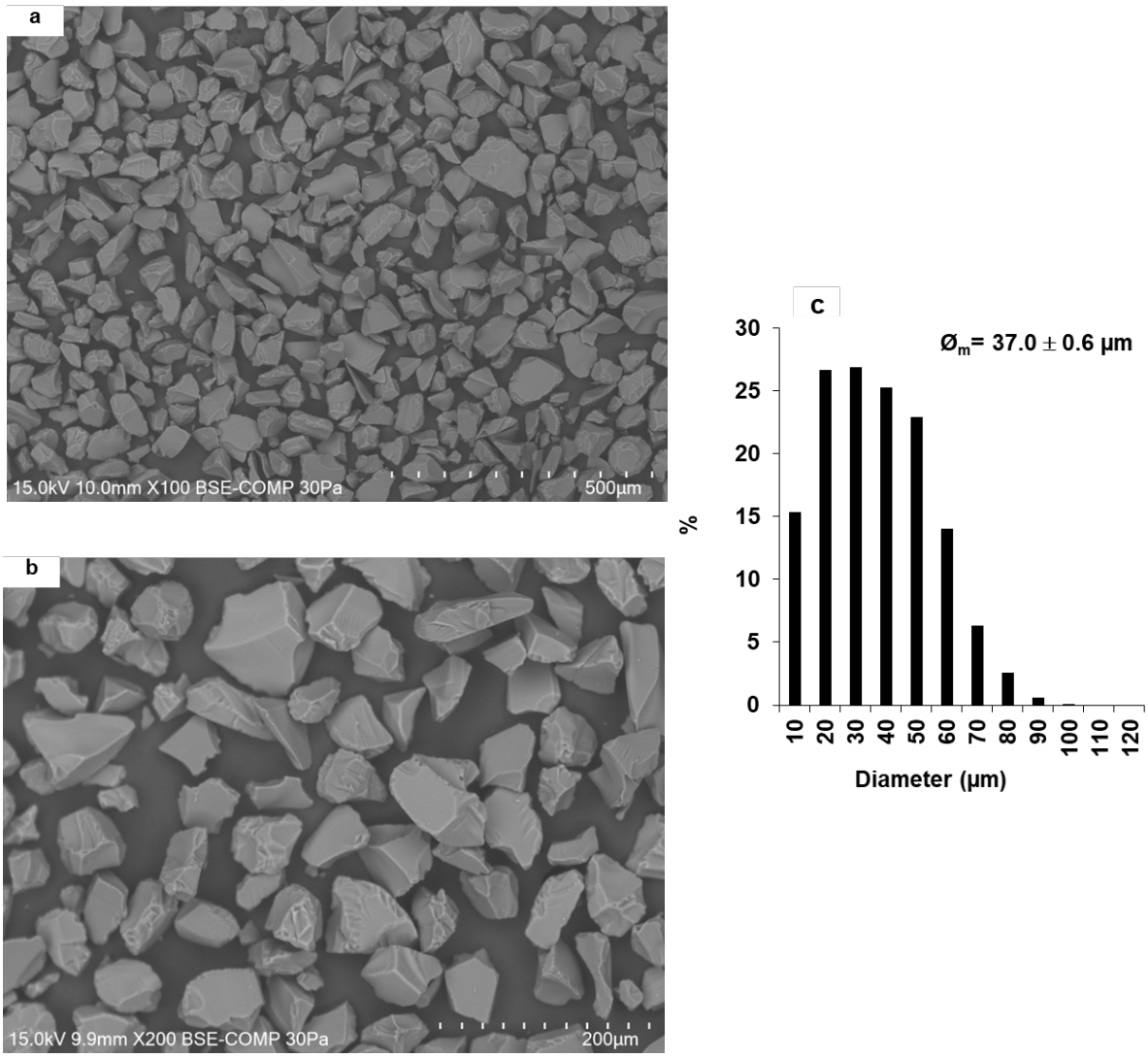

Fig. S4. SEM images of **Rh_10 sample** at a magnification of ×100 (a), × 200 (b), and their particle size distribution (c) determined using Fiji/ImageJ

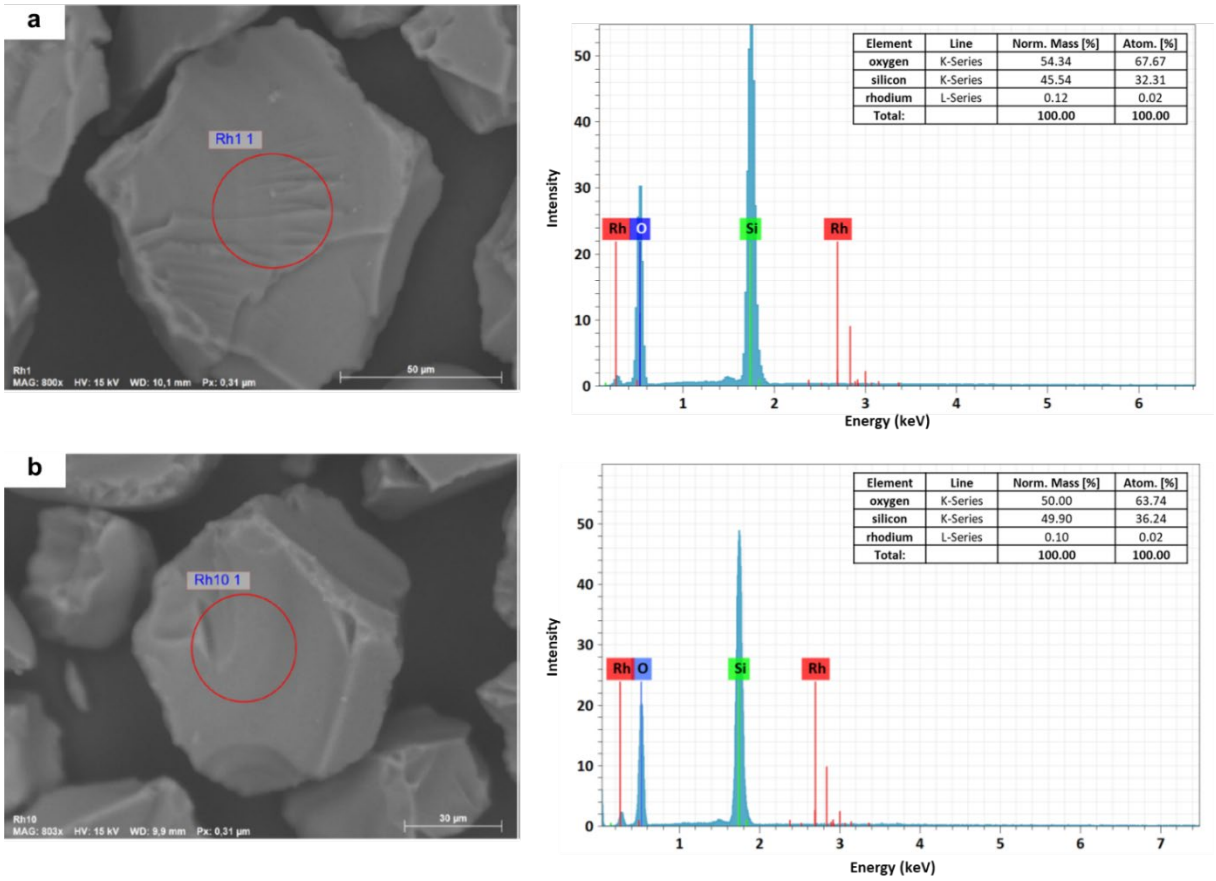

Fig. S5. SEM images of representative grains of **Rh_1** (a) and **Rh_10** (b) showing the analyzed areas and their corresponding EDX elemental spectra

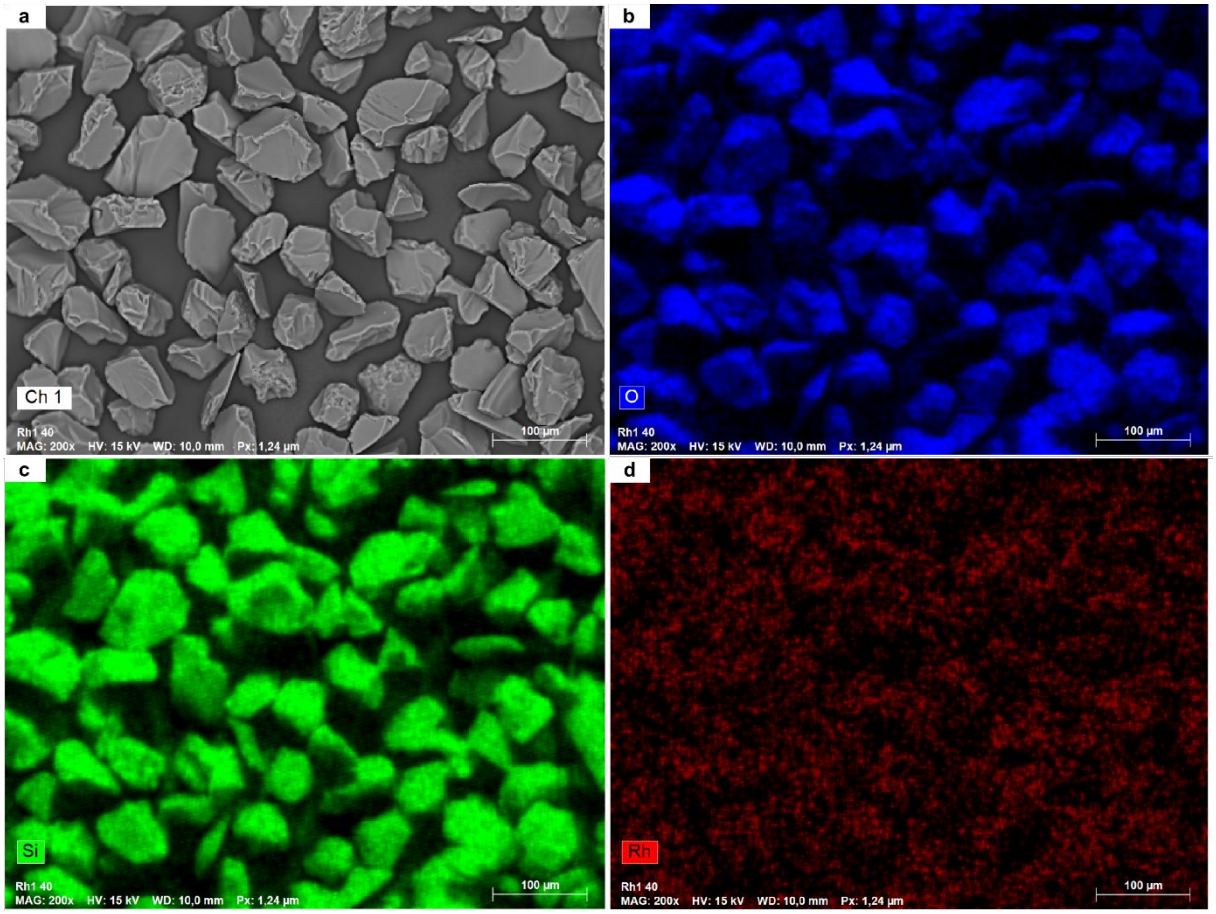

Fig. S6. SEM (a) and EDX (b, c, and d) images of **Rh_1 sample**

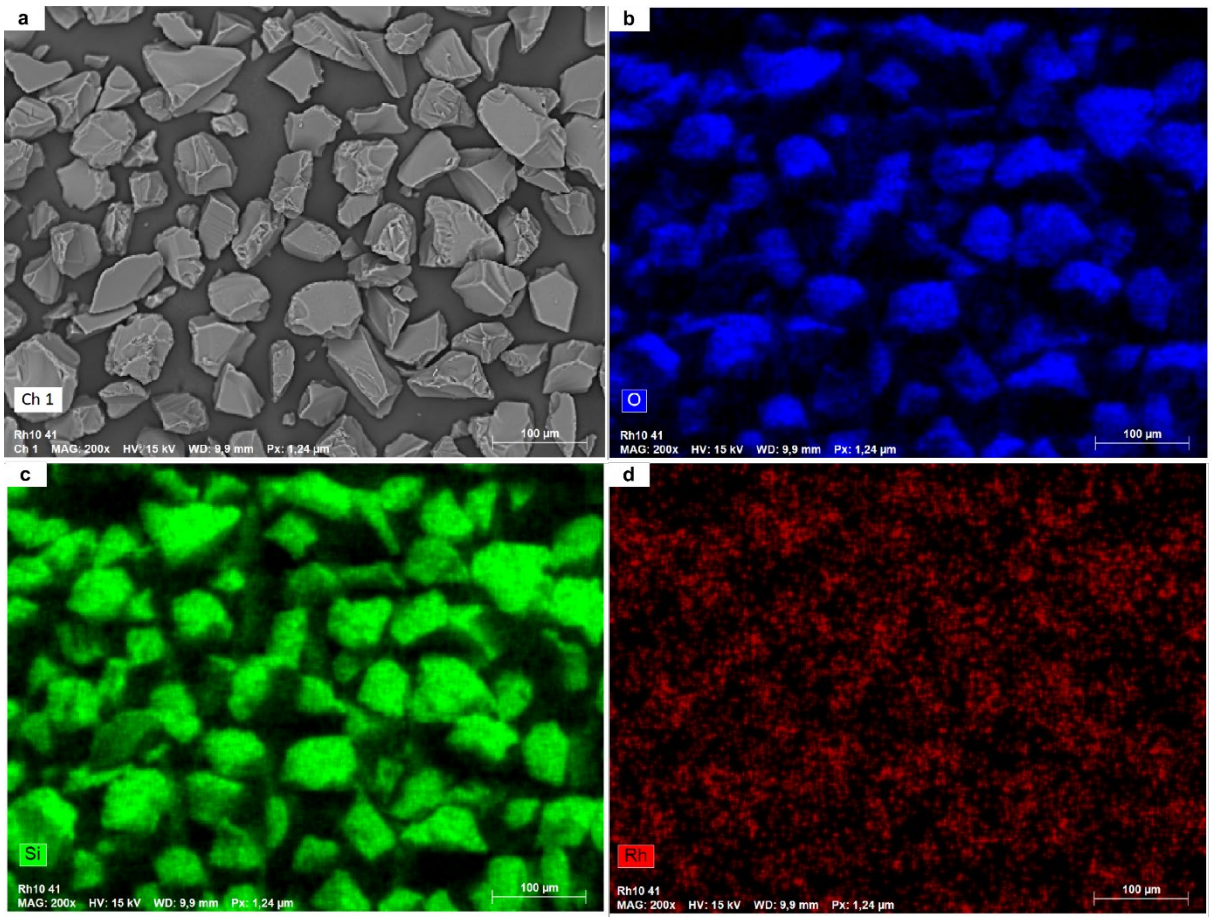

Fig. S7. SEM (a) and EDX (b, c, and d) images of **Rh_10 sample**

12. TEM and HAADF-STEM analysis

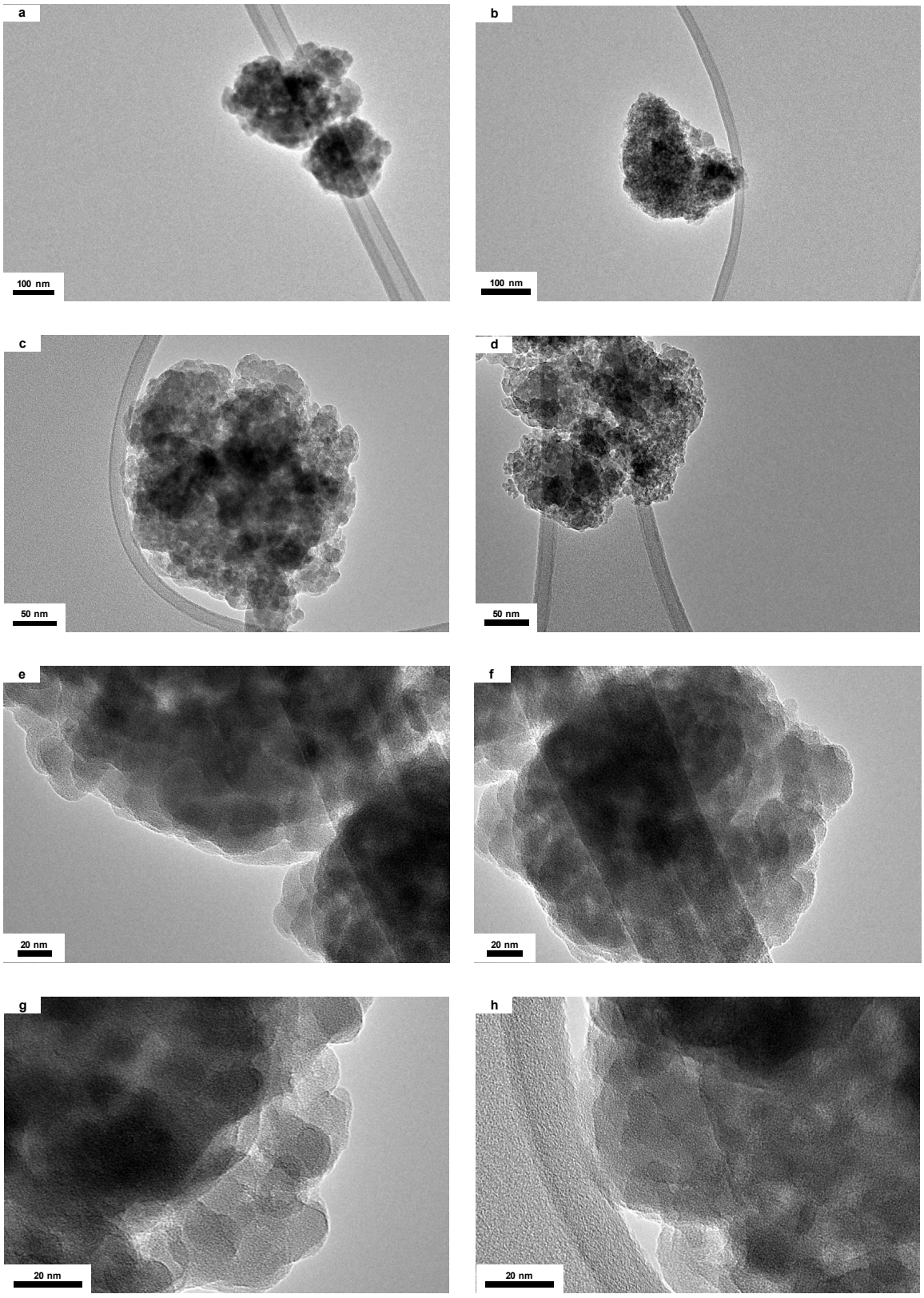

Fig. S8. TEM images of **Rh_1 sample** at a magnification of × 25 000 (a), × 29 000 (b), × 50 000 (c and d), × 100 000 (e and f) and × 200 000 (g and h)

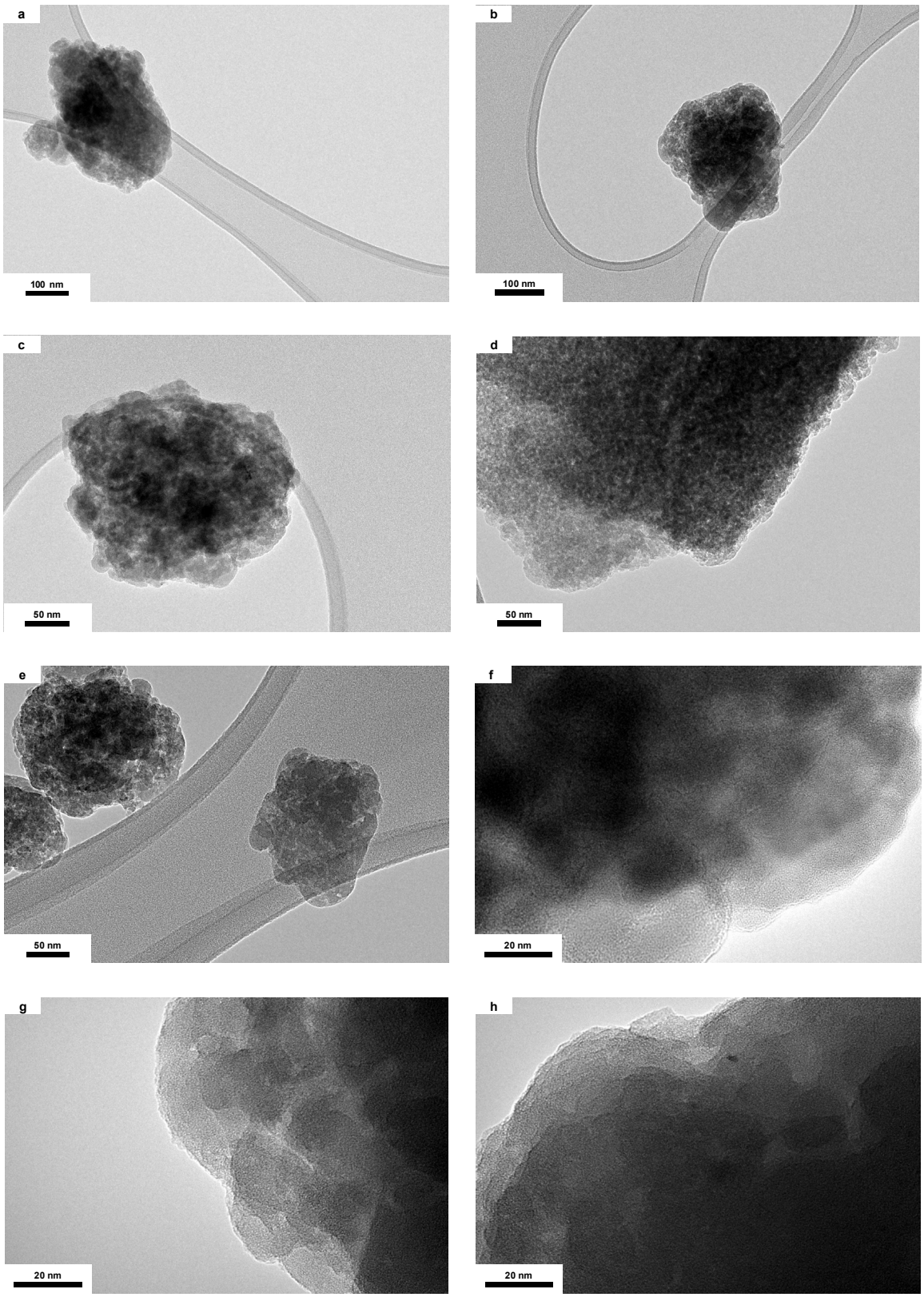

Fig. S9. TEM images of **Rh_10 sample** at a magnification of × 25 000 (a), × 29 000 (b), × 50 000 (c, d and e) and × 200 000 (f, g and h)

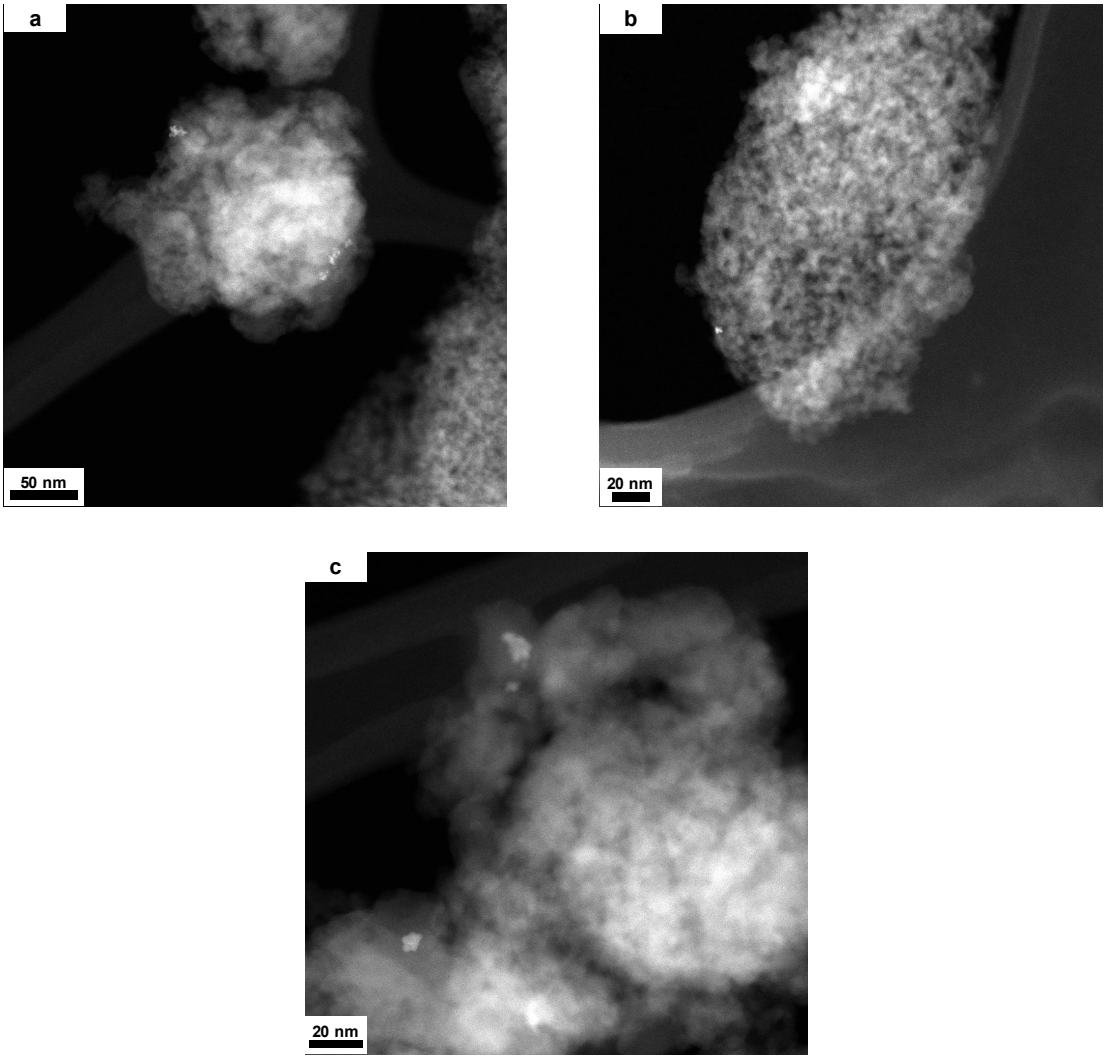

Fig. S10. HAADF-STEM images (a, b and c) of **Rh_1 sample** at different magnification

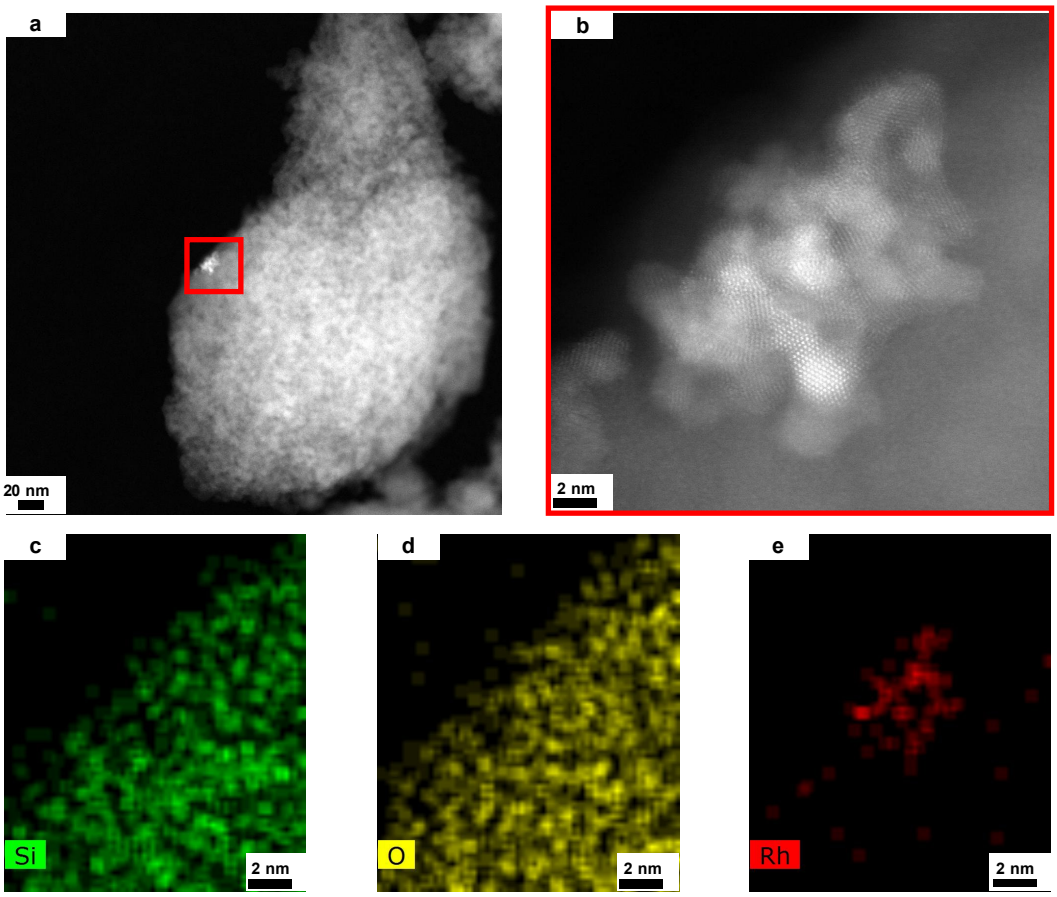

Fig. S11. HAADF-STEM (a and b) and EDX (c, d and e) images of **Rh_1 sample**

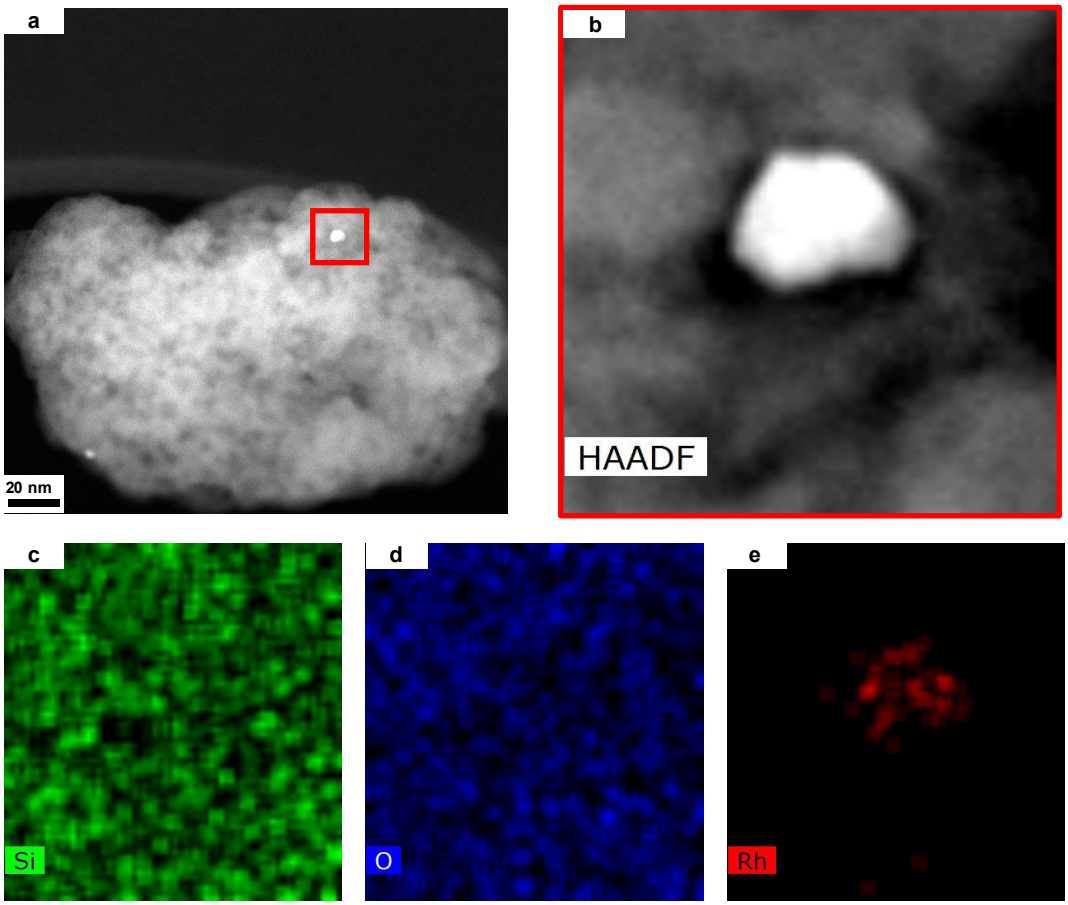

Fig. S12. HAADF-STEM (a and b) and EDX (c, d and e) images of **Rh_10 sample**

13. HAADF-STEM analysis of the thermally treated catalytic material (Rh_TT)

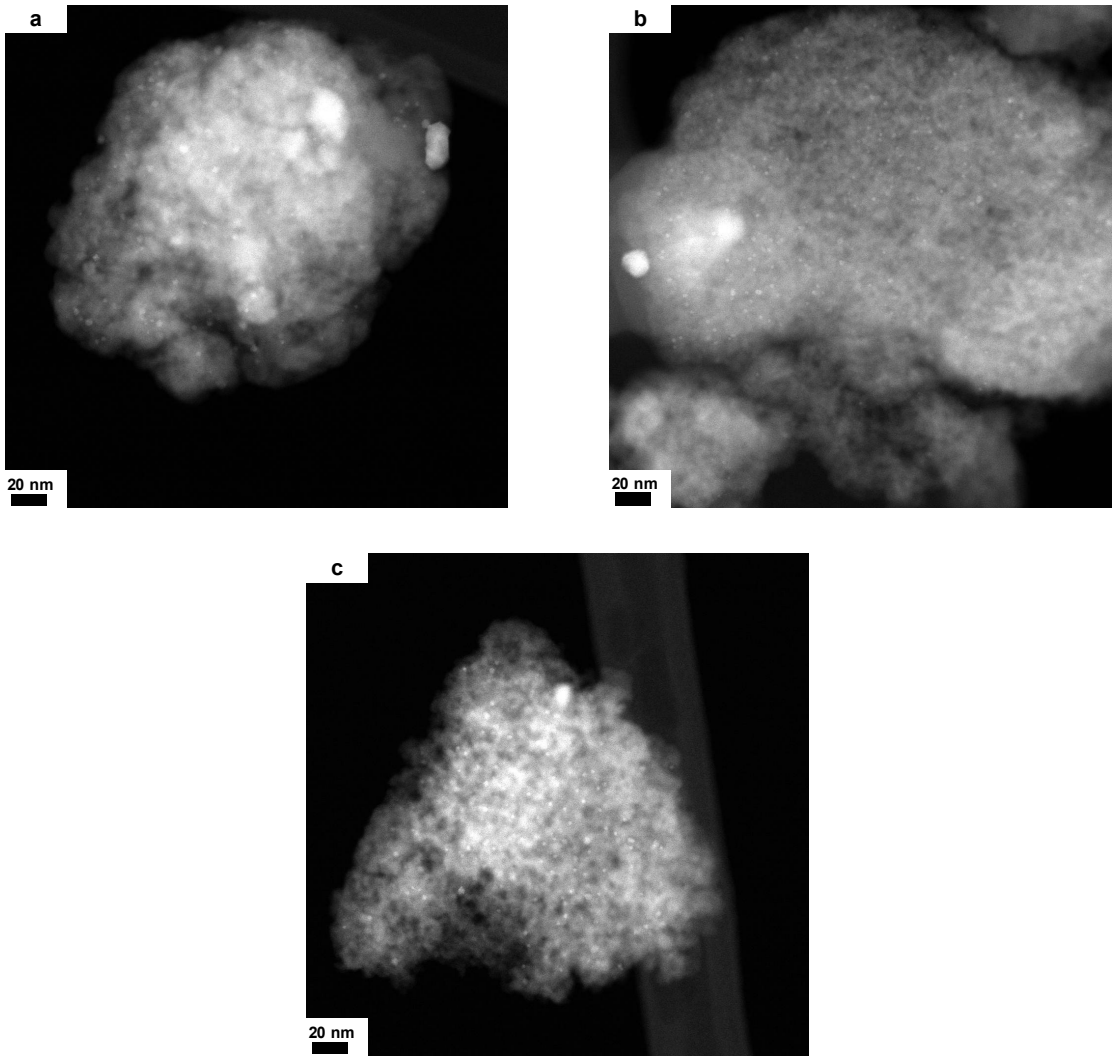

Fig. S13. HAADF-STEM images of **Rh_TT sample**

14. XPS analysis of silica material after the first run (Rh_1)

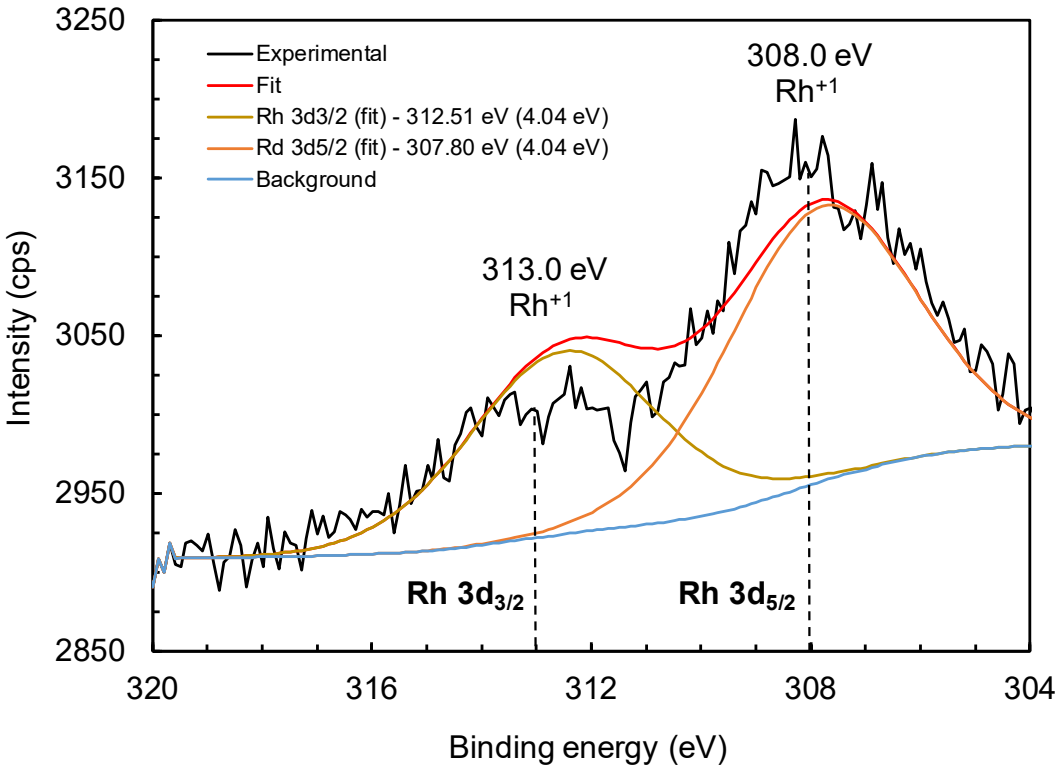

Fig. S14. Rh 3d XPS spectrum of the **Rh_1** sample. The Rh 3d line was deconvoluted by doublets with the GL(30) peak shape. During the fitting procedure the constant values of spin-orbital splitting (4.71 eV) and the Rh 3d5/2/Rh 3d3/2 intensity ratio (1.5) were assumed. The Shirley-type background was applied

15. Evaluation of Rh content in liquid phase

a. Under various conditions

The influence of experimental conditions on catalyst leaching was examined by determining the Rh content in the organic phase for three types of experiments. In the first experiment (Entry 1), after six hours of a **standard reaction**, stirring was stopped and hot filtration (80 °C) was carried out under CO/H_2 pressure (80 bar). In the second experiment (Entry 2), **performed under the same reaction conditions**, stirring was stopped after six hours, the reactor was cooled to room temperature, and cold filtration was conducted under CO/H_2 pressure (80 bar). The third experiment (Entry 3) corresponds to **the standard protocol** used for all studies reported in this work, in which stirring was stopped, the autoclave was cooled to room temperature and then depressurized. After each organic-phase recovery, the Rh content was immediately quantified by ICP-OES spectroscopy.

Table S12. Evaluation of rhodium content in liquid phase under various conditions of a standard reaction[a]

Entry	$P_{CO/H2\ (1:1)}$ (bar)	T (°C)	Rh content[b] (%)
1	80	80	3.0
2	80	25	2.9
3	1	25	3.2

[a]Reaction conditions: $Rh(acac)(CO)_2$: 0.023 mmol (6 mg); TEA: 2.3 mmol (100 eq.); MU: 5.75 mmol (250 eq.); SiO_2 (2 wt% water): 1.2 g; heptane: 10 mL; 6 h. [b]Rh content detected in the liquid phase after reaction.

Note: ICP-OES analysis clearly showed that the Rh percentages (2.9-3.2%) in organic phases were nearly identical in all three cases, regardless of the experimental conditions.

b. At different reaction times

The adsorption of the catalyst during the reaction versus time was evaluated by measuring the Rh content in the organic phase at different time intervals. To this end, a **standard reaction** was carried out under the same experimental conditions described previously. At the selected time points (1, 2, 4, 6, and 24 h), the reactor was cooled to room temperature, depressurized, and the organic phase was decanted, recovered, and immediately analyzed by ICP-OES spectroscopy.

Table S13. Evaluation of rhodium content in liquid phase at different reaction times of a standard reaction[a]

Entry	Time (h)	Rh content[b] (%)
1	1	2.9
2	2	3.1
3	4	3.0
4	6	3.2
5	24	3.3

[a]Reaction conditions: $Rh(acac)(CO)_2$: 0.023 mmol (6 mg); TEA: 2.3 mmol (100 eq.); MU: 5.75 mmol (250 eq.); SiO_2 (2 wt% water): 1.2 g; heptane: 10 mL; 80 °C; 80 bar CO/H_2 (1:1). [b]Rh content detected in the liquid phase after reaction.

Note: The percentage of Rh detected in the liquid phase remained essentially constant (2.9-3.3%) regardless of the reaction time evaluated. The value measured after only 1 h already matches that observed after 24 h, indicating that adsorption onto the solid occurs rapidly. The absence of any significant change over time further demonstrates the remarkable stability of the catalytic species under the studied conditions.

16. Sheldon's hot filtration test

To further investigate the heterogeneity of the Rh/TEA/Silica catalytic system in the reductive hydroformylation reaction, a Sheldon test was performed by separating the catalyst from the reaction liquor after a 1 h primary reaction under the same conditions as the previously reported experiments (**standard reaction**). The resulting filtrate was analyzed by NMR spectroscopy and subsequently subjected to a second reaction by re-feeding syngas for an additional 3 and 12 h, without any added catalyst.

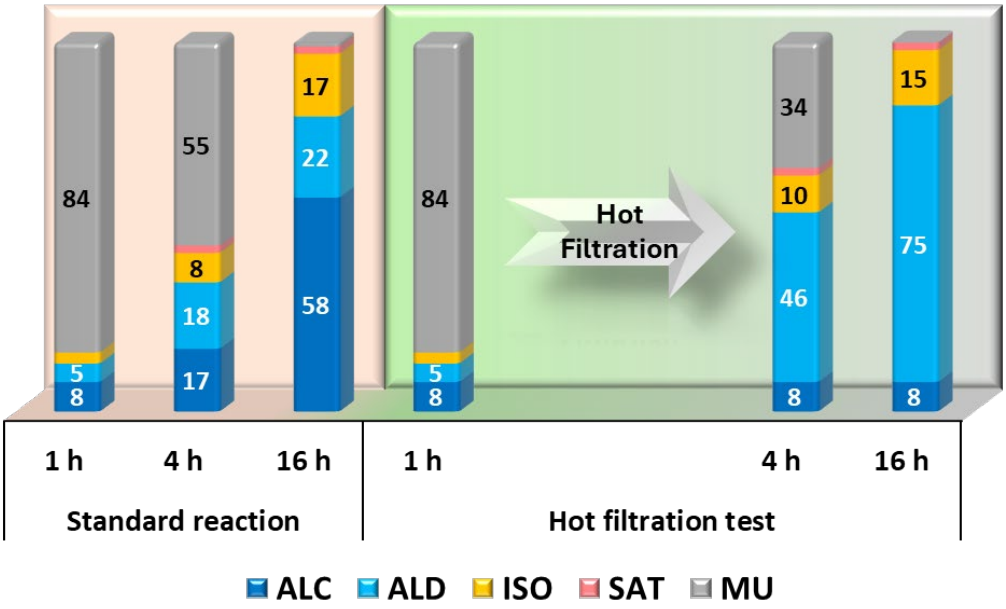

Fig. S15. Catalytic results of the standard reaction and the hot filtration test. Linear-to-branched ratios are reported separately in the following table (**Table S14**).

Table S14. Catalytic results of the standard reaction and the hot filtration test[a]

Experience	Time (h)	Conv.[b] (%)	$Y_{(Ald)}$[c] (%) [*l/b*][d]	$Y_{(Alc)}$[c] (%) [*l/b*][e]	Global [*l/b*][f]	$Y_{(Iso)}$[c] (%)	$Y_{(Sat)}$[c] (%)
Standard reaction	1	16	5 [0.8]	8 [-][g]	[4.0]	3	0
	4	45	18 [1.1]	17 [3.0]	[1.8]	8	2
	16	99	22 [0.4]	58 [2.4]	[1.5]	17	2
Hot filtration test	1	16	5 [0.8]	8 [-][g]	[4.0]	3	0
	4[h]	66	46 [1.7]	8 [-][g]	[2.0]	10	2
	16	100	75 [1.4]	8 [-][g]	[1.6]	15	2

[a]Reaction conditions: $Rh(acac)(CO)_2$: 0.023 mmol (6 mg); TEA: 2.3 mmol (100 eq.); MU: 5.75 mmol (250 eq.); SiO_2 (2 wt% water): 1.2 g; heptane: 10 mL; 80 °C; 80 bar CO/H_2 (1:1). [b]Methyl 10-undecenoate conversion. [c]Y(X) = yield in (X); (Ald) = aldehydes; (Alc) = alcohols; (Iso) = methyl 10-undecenoate isomers; and (Sat) = saturated compound = methyl undecanoate. [d]Linear to branched ratio for aldehydes. [e]Linear to branched ratio for alcohols. [f]Global linear to branched ratio. [g]Only linear alcohols were detected. [h]After separation, the liquid phase was run without the silica support.

Note: Before separation**,** the reaction showed a conversion of 16%, with 5% aldehydes, 8% alcohols, 3% isomers, and no detectable hydrogenation of the double bonds. When the filtrate was re-submitted to syngas at 80 °C for 3 h without adding catalyst, the conversion increased to 66%, yielding 46% aldehydes and 10% isomers, while the alcohol fraction remained unchanged (8%). Extending the reaction by 12 h led to full conversion to aldehydes and isomers, but still without additional alcohol formation. These results suggest that the hydrogenation activity is switched off, within experimental error, after removal of the solid catalyst from the reaction medium**.**

17. Recycling experiments with TEA addition over 6 h ($Rh(acac)(CO)_2$: 0.015 mmol (3 mg), TEA: 2.3 mmol (200 eq.))

To assess the influence of Rh concentration on the recyclability of the Rh/TEA/Silica system, a series of recycling experiments was performed following the first run described in Table S8 (entry 9), each conducted over a 6-hour period with TEA added between each run.

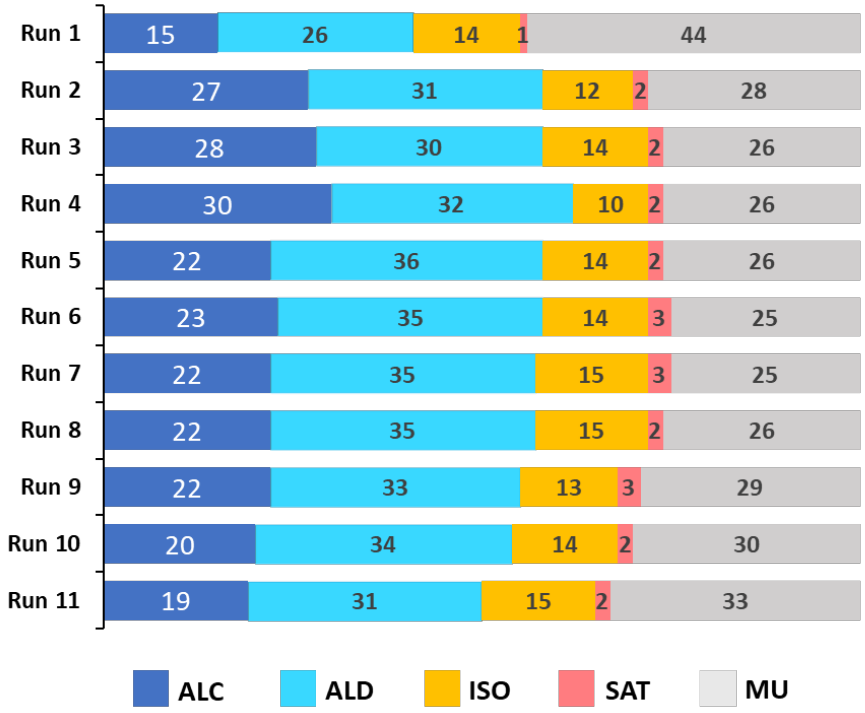

Fig. S16. Catalytic results of recycling experiments with addition of TEA between each run. Linear-to-branched ratios are reported separately in **Table S15**.

Table S15. Catalytic results of recycling experiments with addition of TEA between each run[a]

Run	Conv.[b] (%)	$Y_{(Ald)}$[c] (%) [*l/b*][d]	$Y_{(Alc)}$[c] (%) [*l/b*][e]	Global [*l/b*][f]	$Y_{(Iso)}$[c] (%)	$Y_{(Sat)}$[c] (%)
1	56	26 [1.4]	15 [3.3]	[1.9]	14	1
2	72	31 [1.5]	27 [3.6]	[2.1]	12	2
3	74	30 [1.5]	28 [3.3]	[2.1]	14	2
4	74	32 [1.5]	30 [3.3]	[2.1]	10	2
5	74	36 [1.8]	22 [4.0]	[2.3]	14	2
6	75	35 [1.6]	23 [4.0]	[2.1]	14	3
7	75	35 [1.6]	22 [4.0]	[2.1]	15	3
8	74	35 [1.6]	22 [4.0]	[2.1]	15	2
9	71	33 [1.5]	22 [4.0]	[2.1]	13	3
10	70	34 [1.6]	20 [3.5]	[2.0]	14	2
11	67	31 [1.6]	19 [3.6]	[2.1]	15	2

[a]Reaction conditions for the first run: $Rh(acac)(CO)_2$: 0.015 mmol (3 mg); TEA: 2.3 mmol (200 eq.); MU: 5.75 mmol (250 eq.); SiO_2 (2 wt% water): 1.2 g; heptane: 10 mL; 80 °C; 80 bar CO/H_2 (1:1); 6 h. Run N was conducted with the solid phase of run number N-1, after washing with 3×7 mL of heptane and addition of a fresh mixture of MU (5.75 mmol)/heptane (10 mL)/TEA (2.3 mmol). [b]Methyl 10-undecenoate conversion. [c]Y(X) = yield in (X); (Ald) = aldehydes; (Alc) = alcohols; (Iso) = methyl 10-undecenoate isomers; and (Sat) = saturated compound = methyl undecanoate. [d]Linear to branched ratio for aldehydes. [e]Linear to branched ratio for alcohols. [f]Global linear to branched ratio.

18. Kinetic follow-up of UM reductive hydroformylation in the presence of silica support

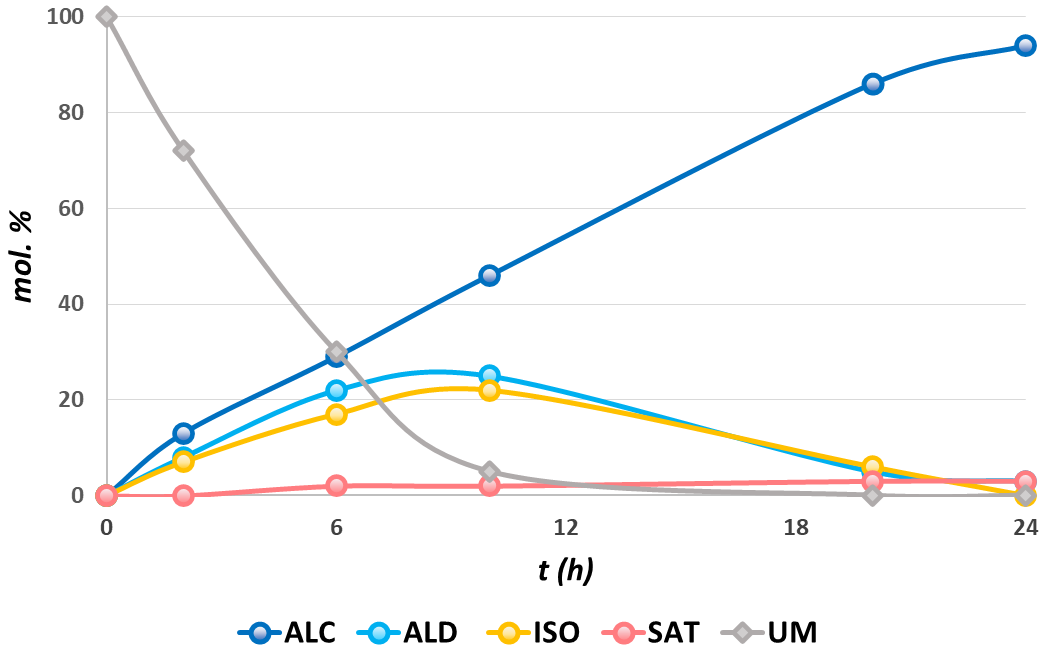

Fig. S17. Kinetic follow-up of UM reductive hydroformylation catalyzed by Rh/TEA/Silica catalytic system. Reaction conditions: $Rh(acac)(CO)_2$: 0.023 mmol (6 mg); TEA: 2.3 mmol (100 eq.); MU: 5.75 mmol (250 eq.); SiO_2 (2 wt% water): 1.2 g; heptane: 10 mL; 80 °C; 80 bar CO/H_2 (1:1).

19. Supplementary Experiences

a. Influence of silica particle size on the HHM reaction and Rh distribution

To further elucidate the role of silica in the reductive hydroformylation reaction pathway, the effect of particle size was examined using silica with a smaller particle size. The silica was mechanically crushed in a planetary ball mill (30 Hz, 10 min) and then tested under the same conditions as the standard reaction.

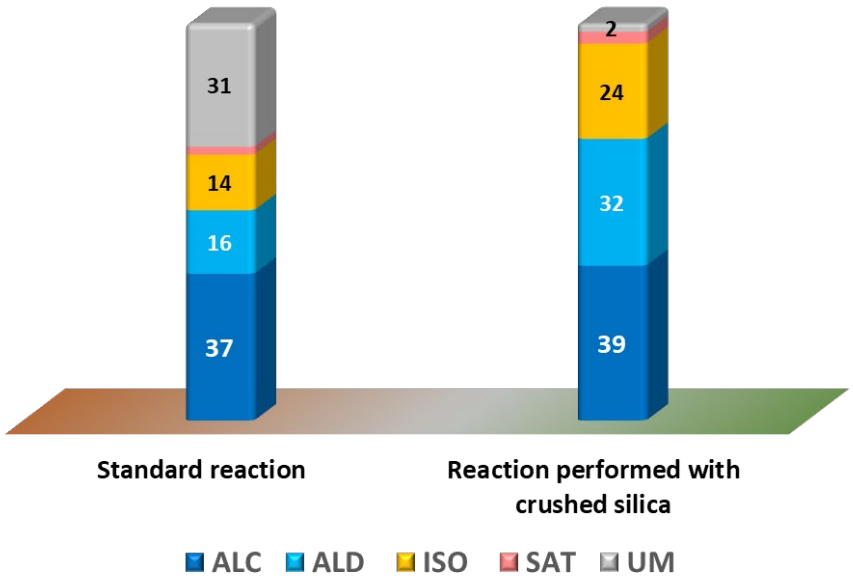

Fig. S18. Comparison of catalytic results obtained with unmodified silica (left) and mechanically crushed silica (right). Rh contents and linear-to-branched ratios are reported separately in **Table S16**.

Table S16. Catalytic results obtained with unmodified silica and mechanically crushed silica[a]

Experience	Conv.[b] (%)	$Y_{(Ald)}$[c] (%) [*l/b*][d]	$Y_{(Alc)}$[c] (%) [*l/b*][e]	Global [*l/b*][f]	$Y_{(Iso)}$[c] (%)	$Y_{(Sat)}$[c] (%)	Rh content[g] (%)
Standard reaction	69	16 [1.1]	37 [3.1]	[1.9]	14	2	3.4
Reaction performed with crushed silica	98	32 [1.1]	39 [3.3]	[2.0]	24	3	5.9

[a]Reaction conditions: $Rh(acac)(CO)_2$: 0.023 mmol (6 mg); TEA: 2.3 mmol (100 eq.); MU: 5.75 mmol (250 eq.); SiO_2 (7.4 wt% water): 1.2 g; heptane: 10 mL; 80 °C; 80 bar CO/H_2 (1:1). [b]Methyl 10-undecenoate conversion. [c]Y(X) = yield in (X); (Ald) = aldehydes; (Alc) = alcohols; (Iso) = methyl 10-undecenoate isomers; and (Sat) = saturated compound = methyl undecanoate. [d]Linear to branched ratio for aldehydes. [e]Linear to branched ratio for alcohols. [f]Global linear to branched ratio. [g]Rh content detected in the liquid phase after reaction.

b. Influence of silica loading

As discussed in the manuscript, the dynamic nature of the catalytic environment under CO/H_2 and in the presence of amines suggests that the silica mass may impact this equilibrium and, consequently, the catalytic performance. Therefore, two silica loadings (0.6 and 2.4 g) were evaluated in the reductive hydroformylation of methyl 10-undecenoate.

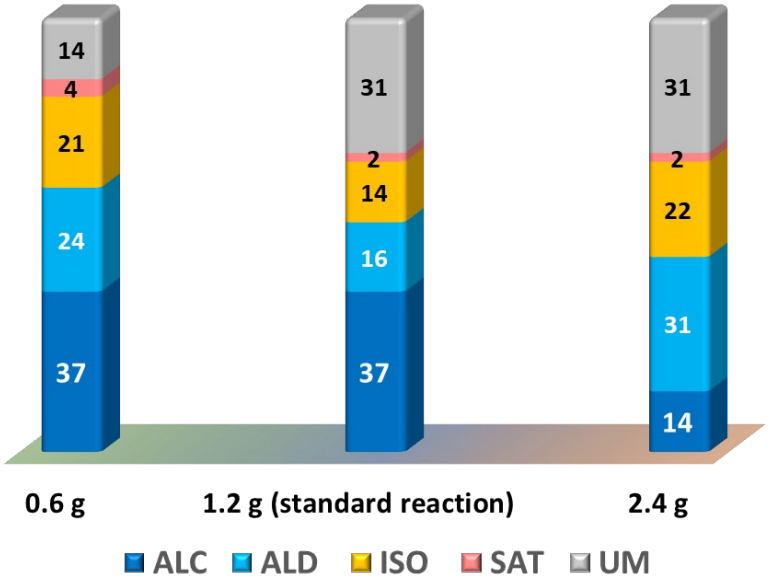

Fig. S19. Comparison of catalytic results obtained with different silica masses. Rh contents and linear-to-branched ratios are reported separately in **Table S17**.

Table S17. Catalytic results obtained with different silica masses[a]

m_{silica} (g)	Conv.[b] (%)	$Y_{(Ald)}$[c] (%) [*l/b*][d]	$Y_{(Alc)}$[c] (%) [*l/b*][e]	Global [*l/b*][f]	$Y_{(Iso)}$[c] (%)	$Y_{(Sat)}$[c] (%)	Rh content[g] (%)
0.6	86	24 [1.2]	37 [3.1]	[2.0]	21	4	4.6
1.2	69	16 [1.1]	37 [3.1]	[1.9]	14	2	3.4
2.4	69	31 [1.5]	14 [3.3]	[1.9]	22	2	5.9

[a]Reaction conditions: $Rh(acac)(CO)_2$: 0.023 mmol (6 mg); TEA: 2.3 mmol (100 eq.); MU: 5.75 mmol (250 eq.); SiO_2 (7.4 wt% water); heptane: 10 mL; 80 °C; 80 bar CO/H_2 (1:1). [b]Methyl 10-undecenoate conversion. [c]Y(X) = yield in (X); (Ald) = aldehydes; (Alc) = alcohols; (Iso) = methyl 10-undecenoate isomers; and (Sat) = saturated compound = methyl undecanoate. [d]Linear to branched ratio for aldehydes. [e]Linear to branched ratio for alcohols. [f]Global linear to branched ratio. [g]Rh content detected in the liquid phase after reaction.

c. Influence of the organic phase volume

Similarly to the solid phase (silica), increasing the volume of the organic phase (heptane) may affect the distribution of Rh between the liquid and solid phases. Accordingly, an experiment was performed with a heptane volume 1.5-fold higher than the standard condition (15 mL).

Table S18. Effect of heptane volume on catalytic performance[a]

$V_{Heptane}$ (mL)	Conv.[b] (%)	$Y_{(Ald)}$[c] (%) [*l/b*][d]	$Y_{(Alc)}$[c] (%) [*l/b*][e]	Global [*l/b*][f]	$Y_{(Iso)}$[c] (%)	$Y_{(Sat)}$[c] (%)	Rh content[g] (%)
10	69	16 [1.1]	37 [3.1]	[1.9]	14	2	3.4
15	88	26 [1.2]	36 [3.5]	[2.1]	24	2	6.0

[a]Reaction conditions: $Rh(acac)(CO)_2$: 0.023 mmol (6 mg); TEA: 2.3 mmol (100 eq.); MU: 5.75 mmol (250 eq.); SiO_2 (7.4 wt% water): 1.2 g; heptane (10 or 15 mL); 80 °C; 80 bar CO/H_2 (1:1). [b]Methyl 10-undecenoate conversion. [c]Y(X) = yield in (X); (Ald) = aldehydes; (Alc) = alcohols; (Iso) = methyl 10-undecenoate isomers; and (Sat) = saturated compound = methyl undecanoate. [d]Linear to branched ratio for aldehydes. [e]Linear to branched ratio for alcohols. [f]Global linear to branched ratio. [g]Rh content detected in the liquid phase after reaction.

II. Experimental and analytical procedures

1. General information

The catalytic precursor $Rh(acac)(CO)_2$ was purchased from Merck and used as received. All amine products were obtained from Fisher Scientific or Merck, except for K-DMT (synthesized from commercial taurine, Fisher Scientific) and PIPMIM-PF_6, which were prepared according to published procedures (see Experimental Section). Methyl 10-undecenoate was supplied by Merck. Heptane, cyrene, γ-valerolactone (GVL), methyl isobutyl ketone (MIBK), 2-methyltetrahydrofuran (2-MeTHF), anisole, dimethyl carbonate (DMC), *p*-cymene, and dodecane were obtained from Acros Organics, Fisher Scientific, or Merck. Pinane solvent was provided by SARL SICO-CHEM and POC SARL (France). Silica material (SiO_2, MW = 60.08 $g \cdot mol^{-1}$, $S_{BET} = 430\ m^2 \cdot g^{-1}$) was provided by Acros Organics. Syngas (CO/H_2, 1:1) was supplied by the Linde Group in cylinders pressurized to 150 bar.

2. Synthesis and characterization of potassium *N,N*-dimethyltaurinate (K-DMT) and PEMIM-PF_6

The synthesis of the K-DMT ligand was carried out following our previously reported procedure [4]. Typically, in a 200 mL round-bottom flask equipped with a magnetic stir bar and a condenser, 4.13 g of taurine (33 mmol), 11.2 g of 37 % formaldehyde (138 mmol), and 7.5 g of 98 % formic acid (160 mmol) were successively added under stirring. The mixture was then heated at 90 °C for 8 h. After concentration of the reaction mixture using a rotary evaporator, the resulting solid was dissolved in 10 mL of water and concentrated again. This operation was repeated twice. The solid was then dissolved once more in a minimal amount of water, frozen in liquid nitrogen, and lyophilized under vacuum. *N,N*-Dimethyltaurine (DMT) was obtained as a white powder (7.75 g, 94 % yield). *N,N*-Dimethyltaurinate (K-DMT) was quantitatively obtained by stirring 1 g of *N,N*-dimethyltaurine with 1 equivalent of KOH in water for 20 min. The resulting aqueous solution was then frozen in liquid nitrogen and lyophilized to afford the solid compound.

PEMIM-PF_6 was prepared according to the method reported in [11]. A solution of *N*-methylimidazole (59 g, 0.71 mol) in 100 mL of ethanol was treated with 1-(2-chloroethyl) piperidine hydrochloride (129 g, 0.70 mol). The reaction mixture was stirred and refluxed for 8 h. After removal of the ethanol and washing with CH_2Cl_2, pale-yellow solids were obtained, corresponding to 1-(2-piperid-1-yl-ethyl)-3-methylimidazolium chloride. These solids were

then mixed with NH_4PF_6 and an aqueous NaOH solution in a 1:1.2:1.2 molar ratio and stirred vigorously at ambient temperature for 24 h. The resulting oily liquid was washed repeatedly with deionized water until the filtrate tested negative with $AgNO_3$. Following extraction with CH_2Cl_2, filtration, and solvent removal, the desired pale-yellow viscous product was obtained (Yield, 42 mol %).

After synthesis, both ligand amines (K-DMT and PEMIM-PF_6) were characterized, and their structures were confirmed by comparison with those reported in the references cited above.

3. Physical-chemical characterization

^{1}H NMR and **^{13}C NMR** spectra were recorded at 298 K on a Bruker Avance Neo 400 NanoBay spectrometer (Wissembourg, France) equipped with a 5 mm SmartProbe BBFO with Z-gradients, operating at 9.4 T field strength (400 MHz for ^{1}H nuclei, and 100 MHz for ^{13}C nuclei). ^{1}H and ^{13}C chemicals shifts were determined using residual signals of the deuterated solvents. Assignment of the signals was carried out using 1D (^{1}H, ^{13}C) and 2D (correlation spectroscopy (COSY), heteronuclear single quantum coherence (HSQC), heteronuclear multiple bond correlation (HMBC) NMR experiments.

Rhodium concentrations were determined by **inductively coupled plasma optical emission spectroscopy (ICP-OES)** using a Thermo Scientific iCAP 7000 Plus Series instrument. Samples consisting of aliquots of the nonpolar phase were digested in a nitric acid medium (70% w/w) prior to analysis by microwave mineralization using a MARS 6 microwave digestion system.

Thermogravimetric analyses (TGA) were carried out on a Mettler Toledo TGA/DSC 3+ instrument to determine the water content of the samples. Approximately 50 mg of each sample were placed in alumina crucibles and heated from 40 °C to 110 °C at a rate of 10 °C min^{-1}, followed by an isothermal step of 20 min at 110 °C under a constant flow of inert gas (N_2) of 50 ml. min^{-1}.

Nitrogen adsorption-desorption measurements were performed on a Micromeritics (Tristar II) surface area and porosity analyzer. Prior to analysis, the samples were degassed under vacuum at 120 °C for 12 h to remove physisorbed moisture and contaminants. Nitrogen isotherms were collected at -196 °C, and the specific surface area (S_{BET}) was calculated using the Brunauer–Emmett–Teller (BET) method. The total porous volume (Vp) was determined at

a relative pressure of P/P_0 = 0.99, and the pore size distribution was obtained from the desorption branch using the Barrett–Joyner–Halenda (BJH) model.

Microstructural observations were performed using a Hitachi SU3800 **scanning electron microscope (SEM)** operated in backscattered electron (BSE) mode, under partial vacuum, at an accelerating voltage of 15 kV and a working distance (WD) of 10 mm. Energy-dispersive X-ray spectroscopy (EDS) analyses were conducted using a Bruker QUANTAX EDS system equipped with an XFlash detector.

Transmission electron microscopy (TEM) was performed on a Tecnai microscope operated at an accelerating voltage of 200 kV. The powder sample was deposited onto a carbon-coated copper grid prior to analysis. **Scanning transmission electron microscopy (STEM)** analysis was performed using a Titan Themis 300 STEM containing a probe aberration corrector and a monochromator with a resolution of 70 pm and an energy resolution of 150 meV. The microscope had a Super-X windowless four-quadrant silicon drift detector for STEM energy-dispersive X-ray (EDX) mapping and annular dark-field detectors. **High-angle annular dark-field (HAADF)** images were collected at scattering angles between 50 and 200 mrad. For grid preparation, a carbon-coated copper grid was dipped in the sample, which was in the form of dried powder. The metal nanoparticle size distribution was determined by measuring approximately 100 nanoparticles randomly selected from different regions of the images using ImageJ software.

The surface analysis was carried out by **X-ray photoelectron spectroscopy (XPS)** using a Kratos Axis Ultra DLD apparatus equipped with a hemi-spherical analyzer and a delay line detector. The spectra were recorded using an Al monochromated X-ray source (10 kV, 15 mA) with a pass energy of 40 eV (0.1 eV·step^{-1}) for high resolution spectra, and a pass energy of 160 eV (1 ev/step) for survey spectrum in hybrid mode and slot lens mode, respectively. The Si 2p binding energy (103.5 eV) was used as the internal reference. Peak fitting and deconvolution of the experimental photopeaks were performed using CasaXPS software.

4. Preparation of thermal treatment of silica

Silica samples treated at 500, 600, and 700 °C were prepared according to a reported procedure for silica calcination [12]. The materials were heated from 20 °C to the target temperature X °C at a rate of 5 °C min^{-1}, followed by an isothermal treatment for 60 min under a nitrogen atmosphere in a tubular furnace, yielding the Silica@X solids.

Unlike the other treated materials, the preparation of Silica@1000 °C was not based on a specific reference procedure. The sample was heated from 20 °C to 1000 °C at a rate of 5 °C min^{-1}, followed by an isothermal step of 60 min in ambient air using a muffle furnace. This treatment was intentionally designed to destroy the silica porosity, as confirmed by BET analysis.

5. Preparation of various hydrated silica

The silica supports with different water contents were prepared using two approaches. First, as the commercial silica contains 7.4 wt% water, samples of this material were dried at 95 and 110 °C to reduce the water content to 2 wt% and 0.6 wt%, respectively. Higher hydration levels (44 wt% and 54 wt%) were achieved by placing a well-dried silica sample on a flat rectangular tray and slowly adding a precise amount of water drop by drop across the entire surface. The material was then transferred to a centrifuge tube and placed on an orbital shaker to ensure uniform distribution of water throughout the pores. The water contents of all samples were confirmed by TGA analysis.

6. Catalytic tests in batch process

All reactions involving metal–amine catalysts were performed under an air atmosphere. The catalytic experiments were conducted under a fume hood in a room equipped with a CO detector and an explosimeter, both connected to an alarm system, using a 25 or 100 mL autoclave (Parr Instrument Company) fitted with a mechanical stirrer. In a typical catalytic experiment, $Rh(acac)(CO)_2$ (6.0 mg, 0,023 mmol, 1 eq.), amine (100 eq., classically), methyl 10-undecenoate (5.81 mmol, 250 eq.), silica material (1,2 g, 2 wt% water), and heptane (10 mL), were added in a 25 mL stainless-steel autoclave. The reactor was sealed; the reaction mixture was stirred at 1000 rpm and heated at 80 °C. Then, the reactor was pressurized with 80 bar of CO/H_2 (1:1). After the appropriate reaction time was reached, the reactor was cooled to room temperature and depressurized. The liquid phase was then separated by decantation, and, after evaporation of heptane, the resulting mixture was analyzed by NMR spectroscopy. The solid layer, which contains the catalyst, can then be used for a subsequent recycling run.

Unlike liquid amines, the solid amines K-DMT and PEMIM-PF_6 must be introduced differently. Indeed, $Rh(acac)(CO)_2$ (6 mg, 1 eq.) was first dissolved in 10 mL of methanol under stirring at room temperature, after which the N-containing ligand (100 eq.) was added. The mixture was stirred for 2 h until a homogeneous solution was obtained. Then, 1.2 g of silica (2 wt% water)

was added, allowing impregnation of the solid support under stirring for an additional 2 h at room temperature. After solvent removal using a rotary evaporator, the impregnated solid was dried at 65 °C overnight. From this point onward, the same experimental protocol was applied as for the other amines.

7. Recycling experiments without amine addition

After separation from the liquid phase, the solid support layer containing the catalytic system was washed three times with 7 mL of heptane and subsequently dried in air to remove residual solvent. A fresh mixture of methyl 10-undecenoate and heptane was then introduced. A control sample was systematically withdrawn before each new run and analyzed by ^{1}H NMR spectroscopy to determine whether residual products remained on solid support. After the appropriate reaction time was reached, the reactor was cooled to room temperature and depressurized. The liquid phase was then separated by decantation, and, after evaporation of heptane, the resulting mixture was analyzed by NMR spectroscopy.

8. Recycling experiments with amine addition

The same procedure described above was applied for these experiments, except that amine was added before each recycling run (100 eq. with respect to the amount of Rh introduced in the first run). A control sample was systematically withdrawn before each new run and analyzed by ^{1}H NMR spectroscopy to determine whether residual products remained on solid support. After the appropriate reaction time was reached, the reactor was cooled to room temperature and depressurized. The liquid phase was then separated by decantation, and, after evaporation of heptane, the resulting mixture was analyzed by NMR spectroscopy.

9. Determination of conversion, yields, and l/b ratios for the catalytic experiments

Conversions, product yields, and linear/branched (l/b) ratios were determined from NMR spectra. All calculations followed the methodology reported in our previous work [4] using the same substrate, methyl 10-undecenoate (UM).

III. References

[1] D. N. Gorbunov, M. V. Nenasheva, E. A. Kuvandykova, S. V. Kardashev, and E. A. Karakhanov, 'Promising Applications of Polyethyleneimine as a Ligand in Rhodium-Catalyzed Tandem Hydroformylation/Hydrogenation of Olefins', *Pet. Chem.*, vol. 63, no. 5, pp. 594–606, May 2023, doi: 10.1134/S0965544123030222.

[2] M. Nenasheva, D. Gorbunov, M. Karasaeva, A. Maximov, and E. Karakhanov, 'Non-phosphorus recyclable Rh/triethanolamine catalytic system for tandem hydroformylation/hydrogenation and hydroaminomethylation of olefins under biphasic conditions', *Mol. Catal.*, vol. 516, p. 112010, Nov. 2021, doi: 10.1016/j.mcat.2021.112010.

[3] S. Püschel, E. Hammami, T. Rösler, K. R. Ehmann, A. J. Vorholt, and W. Leitner, 'Auto-tandem catalytic reductive hydroformylation with continuous multiphase catalyst recycling', *Catal. Sci. Technol.*, vol. 12, no. 3, pp. 728–736, 2022, doi: 10.1039/D1CY02000E.

[4] A. El Mouat *et al.*, 'Promising Recyclable Ionic Liquid-Soluble Catalytic System for Reductive Hydroformylation', *ACS Sustain. Chem. Eng.*, vol. 10, no. 34, pp. 11310–11319, Aug. 2022, doi: 10.1021/acssuschemeng.2c03302.

[5] A. El Mouat *et al.*, 'Rhodium/Trialkylamines Catalyzed Reductive Hydroformylation in Ionic Liquid/Heptane Medium: An Unexpected Concept for Catalyst Recycling in Batch and Continuous Flow Processes', *ChemSusChem*, vol. 18, no. 3, p. e202401384, Feb. 2025, doi: 10.1002/cssc.202401384.

[6] L. Alvila, T. A. Pakkanen, T. T. Pakkanen, and O. Krause, 'Hydroformylation of olefins catalysed by rhodium and cobalt clusters supported on organic (Dowex) resins', *J. Mol. Catal.*, vol. 71, no. 3, pp. 281–290, Feb. 1992, doi: 10.1016/0304-5102(92)85019-C.

[7] L. Alvila, T. A. Pakkanen, T. T. Pakkanen, and O. Krause, 'Catalytic hydroformylation of 1-hexene over $Co_2Rh_2(CO)_{12}$ supported on inorganic carrier materials'.

[8] B. Corain *et al.*, 'Direct synthesis of alcohols from n-olefins and syngas in the liquid phase catalyzed by rhodium supported on crosslinked acrylic resins', *J. Mol. Catal.*, vol. 73, no. 1, pp. 23–41, Apr. 1992, doi: 10.1016/0304-5102(92)80059-P.

[9] D. Gorbunov, M. Nenasheva, E. Naranov, A. Maximov, E. Rosenberg, and E. Karakhanov, 'Tandem hydroformylation/hydrogenation over novel immobilized Rh-containing catalysts based on tertiary amine-functionalized hybrid inorganic-organic

materials', *Appl. Catal. Gen.*, vol. 623, p. 118266, Aug. 2021, doi: 10.1016/j.apcata.2021.118266.

[10] K. V. A. Birkelbach *et al.*, 'An Immobilized Rh-Based Solid Molecular Catalyst for the Reductive Hydroformylation of 1-Octene', *Angew. Chem. Int. Ed.*, vol. 64, no. 33, p. e202424144, Aug. 2025, doi: 10.1002/anie.202424144.

[11] Q.-X. Wan, Y. Liu, Y. Lu, M. Li, and H.-H. Wu, 'Palladium-Catalyzed Heck Reaction in the Multi-Functionalized Ionic Liquid Compositions', *Catal. Lett.*, vol. 121, no. 3, pp. 331–336, Mar. 2008, doi: 10.1007/s10562-007-9343-y.

[12] A. Oufakir and L. Khouchaf, 'Structural and Surface Changes of SiO2 Flint Aggregates under Thermal Treatment for Potential Valorization', *Crystals*, vol. 13, no. 4, p. 647, Apr. 2023, doi: 10.3390/cryst13040647.